


Cell Surface Calcium-Sensing Receptor Heterodimers: Mutant Gene Dosage Affects Ca^{2+} Sensing but Not G Protein Interaction

Mahvash A. Goolam,¹ Alice P. Brown,¹ Kimberly T. Edwards,¹ Karen J. Gregory,² Katie Leach,² and Arthur D. Conigrave¹ 

¹School of Life and Environmental Sciences, Charles Perkins Centre (D17), University of Sydney, NSW, Australia

²Monash Institute of Pharmaceutical Sciences and Department of Pharmacology, Monash University, Parkville, Victoria, Australia

ABSTRACT

The calcium-sensing receptor is a homodimeric class C G protein-coupled receptor (GPCR) that senses extracellular Ca^{2+} (Ca^{2+}_o) via a dimeric extracellular Venus flytrap (VFT) unit that activates G protein-dependent signaling via twin Cysteine-rich domains linked to transmembrane heptahelical (HH) bundles. It plays a key role in the regulation of human calcium and thus mineral metabolism. However, the nature of interactions between VFT units and HH bundles, and the impacts of heterozygous or homozygous inactivating mutations, which have implications for disorders of calcium metabolism are not yet clearly defined. Herein we generated CaSR-GABA_{B1} and CaSR-GABA_{B2} chimeras subject to GABA_B-dependent endoplasmic reticulum sorting to traffic mutant heterodimers to the cell surface. Transfected HEK-293 cells were assessed for Ca^{2+}_o -stimulated Ca^{2+}_i mobilization using mutations in either the VFT domains and/or HH bundle intraloop-2 or intraloop-3. When the same mutation was present in both VFT domains of receptor dimers, analogous to homozygous neonatal severe hyperparathyroidism (NSHPT), receptor function was markedly impaired. Mutant heterodimers containing one wild-type (WT) and one mutant VFT domain, however, corresponding to heterozygous familial hypocalciuric hypercalcemia type-1 (FHH-1), supported maximal signaling with reduced Ca^{2+}_o potency. Thus two WT VFT domains were required for normal Ca^{2+}_o potency and there was a pronounced gene-dosage effect. In contrast, a single WT HH bundle was insufficient for maximal signaling and there was no functional difference between heterodimers in which the mutation was present in one or both intraloops; ie, no gene-dosage effect. Finally, we observed that the Ca^{2+}_o -stimulated CaSR operated exclusively via signaling *in-trans* and not via combined *in-trans* and *in-cis* signaling. We consider how receptor asymmetry may support the underlying mechanisms. © 2022 The Authors. *Journal of Bone and Mineral Research* published by Wiley Periodicals LLC on behalf of American Society for Bone and Mineral Research (ASBMR).

KEY WORDS: G protein-coupled receptor (GPCR); calcium; class C GPCR; calcium-sensing receptor; heterotrimeric G protein; calcium intracellular release; cell culture; mutant heterodimers; GABA_B sorting system; signaling *in-trans*

Introduction

G protein coupled receptors (GPCRs) control key cell functions and cell fate, and also contribute to the control of whole body metabolism (reviewed in Refs. 1-4). The extracellular Ca^{2+}_o -sensing receptor (CaSR) is a class C GPCR that plays key roles in support of calcium homeostasis and mineral metabolism (reviewed in Refs. 5-7). In two key functions it mediates Ca^{2+}_o -dependent feedback inhibition of parathyroid hormone (PTH) secretion and renal calcium reabsorption (reviewed in Ref. 8). The CaSR's sensitivity to small changes in Ca^{2+}_o is exquisite in

tissues in which it is expressed at the highest levels, including cells of the parathyroid gland and renal cortical thick ascending limb (reviewed in Ref. 9).

The CaSR is a pleiotropic GPCR, which upon Ca^{2+}_o binding activates various downstream signaling pathways dependent upon coupling to distinct G proteins and other signaling proteins.⁽⁸⁾ These include G_{q/11}-dependent Ca^{2+}_i signaling mediated in part via the activation of phosphoinositide-specific phospholipase C (PI-PLC), G_{i/o}-mediated suppression of cyclic adenosine monophosphate (cAMP) synthesis, and phosphorylation of several important intracellular protein kinases including protein

This is an open access article under the terms of the [Creative Commons Attribution-NonCommercial-NoDerivs](https://creativecommons.org/licenses/by-nc-nd/4.0/) License, which permits use and distribution in any medium, provided the original work is properly cited, the use is non-commercial and no modifications or adaptations are made.

Received in original form December 14, 2020; revised form June 20, 2022; accepted July 14, 2022.

Address correspondence to: Arthur D. Conigrave, MD, PhD, School of Life and Environmental Sciences, Charles Perkins Centre (D17), University of Sydney, New South Wales, 2006, Australia. E-mail: arthur.conigrave@sydney.edu.au

Additional Supporting Information may be found in the online version of this article.

Journal of Bone and Mineral Research, Vol. 37, No. 9, September 2022, pp 1787–1807.

DOI: 10.1002/jbmr.4651

© 2022 The Authors. *Journal of Bone and Mineral Research* published by Wiley Periodicals LLC on behalf of American Society for Bone and Mineral Research (ASBMR).

kinase C (PKC) and extracellular signal-regulated kinase 1/2 (ERK_{1/2}) (reviewed in Ref. 10). The molecular mechanisms that support the activation of these signaling pathways are not well understood. However, recent work suggests that each CaSR homodimer couples to only one heterotrimeric G protein at a time,⁽¹¹⁾ similar to metabotropic glutamate receptors (mGlu)^(12,13) and a recent report that a near-to-full length cryogenic electron microscopy (cryoEM) structure of the activated CaSR exhibits asymmetry in the transmembrane domains of neighboring subunits, appears to support this concept.⁽¹⁴⁾

Like many members of GPCR class C, the CaSR is composed of four main protein domains in tandem: an N-terminal extracellular module comprising a Venus flytrap (VFT) domain linked via an interdomain disulfide to a Cysteine-rich (CR) domain; a heptahelical (HH) bundle comprising seven trans-membrane helices along with three intracellular loops and three extracellular loops; and a cytoplasmic C-terminal domain (reviewed in Ref. 15).

Class C GPCRs are functionally active as dimers (reviewed in Ref. 16). In some cases the receptors are homodimers composed of identical subunits, including the CaSR,⁽¹⁷⁾ mGlu receptors,⁽¹⁸⁾ and GPRC6A.⁽¹⁹⁾ Crystal and cryoEM structures of the extracellular domains of various mGlu receptors have confirmed their organization into homodimers and extracellular disulfides that stabilize subunit interactions have been identified^(20,21). Recently determined crystal structures of the extracellular domain of the CaSR have demonstrated that it also forms homodimers stabilized by a single disulfide 129–129' between neighboring subunits, S and S'^(22,23) and this has also been observed in near-to-full length cryoEM structures of the CaSR.⁽¹⁴⁾

Unlike the examples provided above, several other class C GPCRs such as the GABA_B (GABA_{B1}/GABA_{B2}) receptor and the umami (T1R₁/T1R₃) and sweet (T1R₂/T1R₃) taste receptors are obligate heterodimers composed of two distinct subunits that preferentially associate in the endoplasmic reticulum (ER) lumen following translation and translocation (reviewed in Ref. 16). In the case of GABA_B receptors, the association of subunits in the ER is critical to function because GABA_{B1} contains an ER retention motif in its C-terminus (*RSRR*; residues 922–925 in the mouse isoform; GenBank AAD22194.2) that, in the absence of the GABA_{B2} subunit, prevents its forward trafficking.^(24–26) When co-expressed with GABA_{B2}, however, GABA_{B1} is released from the ER as a GABA_{B1}-GABA_{B2} heterodimer mediated by a protein-protein interaction in which a coiled-coil domain in the C-terminus of GABA_{B2} masks the ER retention motif.⁽²⁶⁾

Although a number of dimeric structures of class C GPCRs including the CaSR VFT domain⁽²²⁾ and entire extracellular domain,⁽²³⁾ and more recently the near-to-full length CaSR⁽¹⁴⁾ have been determined, the molecular mechanisms that govern receptor-mediated signaling in response to agonists and allosteric modulators are not well defined. The neighboring VFT domains of mGlu receptors act in tandem to control the relative orientations of the dimeric HH bundles (reviewed in Ref. 18); this has also been reported more recently for the CaSR.^(14,23) Consistent with this, glutamate activation of mGlu₂ was only observed in full-length dimeric receptor constructs.⁽¹²⁾ On the other hand, ligands that bind exclusively to the receptor's HH bundles induce them to bind and activate G proteins,⁽¹²⁾ indicating that *in-trans* signaling arises at the level of the disulfide-coupled dimeric VFT units, which control the relative orientations and distance between neighboring CR domains. This leads to a number of questions about CaSR function, recognizing that the chief physiological activator of the CaSR, Ca²⁺, unlike the chief physiological activator of mGlu receptors, glutamate, does *not* bind in the

VFT domain's interdomain cleft but rather at four distinct sites on its surface.⁽²³⁾

In addition, the impacts of heterozygous and homozygous mutations in the VFT sensing domains and HH bundle signaling units are not well understood. Early studies of this question by genetic analysis⁽²⁷⁾ and by plasmid-dependent expression in HEK-293 cells *in vitro*^(28,29) concluded that gene dosage effects can explain the difference in the severity between the benign heterozygous disorder FHH (now known as FHH type-1⁽³⁰⁾) and the more serious, typically homozygous disorder of mineral metabolism, neonatal severe hyperparathyroidism (NSHPT). However, the scope of the behavior with respect to distinct extracellular and intracellular protein domains of the receptor was unclear, and the analysis was based on the co-expression *in vitro* of unmodified CaSR subunits that did not selectively form mutant heterodimers.^(28,29) Instead three dimeric receptor populations coexisted in unknown proportions within the same cell including wild-type (WT) homodimers, mutant homodimers, and heterodimers composed of one WT and one mutant subunit.

Based on the foregoing, two key questions are:

- i. How many functional VFT domains are required for Ca²⁺_o sensing and what are the impacts of heterozygous and homozygous mutations?
- ii. How many functional HH bundles are required for Ca²⁺_o-stimulated signaling and what are the impacts of heterozygous and homozygous mutations of the G protein interacting domains?

Experiments in which HEK-293 cells are transfected either singly or in combination with one of two mutant CaSRs, in which one subunit is defective in its ligand-binding VFT domain and the other is defective in a key intracellular signaling domain, have clarified the dimeric nature of CaSR function and demonstrate that it can operate *in-trans*,^(11,17) as reported for other class C GPCRs (reviewed in Ref. 16). When efficiently expressed and trafficked to the cell surface, CaSR *homodimers* containing either (i) a loss-of-function VFT domain mutation; or (ii) a loss-of-function HH bundle mutation are unresponsive to ligands; ie, mutant homodimers are nonfunctional. However, when co-transfected, CaSR *heterodimers* bearing a loss-of-function VFT domain mutation in one subunit as well as a loss-of-function HH bundle mutation in the other subunit are frequently complementary, exhibiting restored function as demonstrated by Ca²⁺_o-dependent Ca²⁺_i mobilization or inositol monophosphate (IP₁) accumulation.^(11,17)

The requirements of receptor function can be assessed further by introducing additional mutations. However, because of the need to position mutations in one ligand-sensing and in one signaling domain of complementary subunits it is not possible to compare differences in receptor function arising from the presence of heterozygous versus homozygous mutations in either the ligand-sensing or signaling domains. A further limitation is an inability to assess whether normal dimeric CaSR signaling is supported by signaling *in-cis* (ie, within a single subunit) as well as signaling *in-trans* (between subunits).

Kniazeff and colleagues⁽³¹⁾ described tight control of heterodimeric class C GPCRs using complementary chimeras designed to utilize the GABA_B C-terminal ER sorting system. First they made complementary mGlu₅-GABA_{B1} and mGlu₅-GABA_{B2} constructs and then introduced single inactivating mutations into one of the major domains of the mGlu₅-GABA_{B2} constructs to limit receptor function from mGlu₅-GABA_{B2} homodimers. HEK-293

cells were then transfected with these mGlu₅-GABA_{B1} and mGlu₅-GABA_{B2} constructs either singly or in combination. They found that although one intact WT VFT domain was sufficient for receptor function, two WT VFT domains were required for maximum signaling responses.⁽³¹⁾ This GABA_B C-terminus sorting system also permitted analysis of the comparative importance of signaling *in-trans* and *in-cis*. A similar approach has been used to study allostery *in-trans* across the CaSR HH bundle.⁽³²⁾

Herein, we used a GABA_B ER sorting system analogous to that described⁽³¹⁾ to generate CaSR-GABA_{B1} and CaSR-GABA_{B2} chimeras to determine the VFT and signaling domain requirements for Ca²⁺_o-stimulated, CaSR-mediated Ca²⁺_i signaling. In the case of signaling domain requirements we focused on the roles of intraloop-2 and intraloop-3 (iL-2 and iL-3), which are critical for G protein-dependent function.^(33,34) We used recognized inactivating mutations in the VFT domains (G143E and R185Q) and HH bundles (F706A in iL-2, and L797A in iL-3). Finally, we assessed whether Ca²⁺_o-stimulated Ca²⁺_i signaling operates in part by an *in-cis* mechanism as well as the *in-trans* mechanism as reported.^(11,17) We also investigated the behavior of CaSR-mediated activation of phosphatidylinositol-specific phospholipase C (PI-PLC) and its sensitivity to the G_{q/11} inhibitor YM-254890.

Materials and Methods

Cell culture and transfection

HEK-293 cells were cultured in Dulbecco's Modified Eagle's Medium (DMEM) supplemented with 10% fetal bovine serum (FBS), and penicillin (25 U/mL)-streptomycin (25 µg/mL; Thermo-Fisher, Macquarie Park, NSW Australia). Cultures were maintained in a humidified incubator (37°C, 5% CO₂) and subcultured by incubation with 0.25% Trypsin-EDTA (Thermo-Fisher, Macquarie Park, NSW Australia) then washed by centrifugation in fresh DMEM/10% FBS and plated. Upon reaching 70%–95% confluency, subcultured HEK-293 cells were transfected using XtremeGENE HP transfection reagent (Roche, Germany). Briefly, 0.5–1 µg of plasmid DNA was diluted in 100 µL of DMEM (containing 3 µL of transfection reagent) and complexes were allowed to form spontaneously for 15 minutes at room temperature (RT). The complexed solution was added to cell cultures at a final concentration of 9.1% (vol/vol) and the cultures were maintained for 48 hours prior to biochemical and functional analyses. For single transfections, 0.5 µg of DNA was used. For co-transfections, 1.0 µg of DNA was used (0.5 µg per sample).

Molecular biology

Plasmids

WT human CaSR cDNA (WTCaSR; cassette version⁽²⁹⁾) cloned between *Kpn* I and *Xba* I sites of the pcDNA3.1 (+) plasmid was a kind gift from Dr. Mei Bai and Prof. Edward Brown (Endocrine-Hypertension Division, Brigham and Women's Hospital, Boston, MA, USA). pcDNA3.1(+)-WTCaSR(FLAG), which contains the FLAG epitope DYKDDDDK inserted between CaSR residues 371 and 372,⁽³⁵⁾ or pcDNA5/FRT/TO-WTCaSR(Myc), which contains the c-Myc epitope EQKLISEEDL, inserted between CaSR residues 371 and 372,⁽³⁶⁾ were used to generate constructs whose expression could be readily determined by enzyme-linked immunosorbent assay (ELISA) or fluorescence microscopy.

WT mouse GABA_{B1} (GenBank AF114168.2) and human GABA_{B2} (GenBank NP_005449.5) complementary DNAs (cDNAs) were the kind gift of Dr. David Hampson (Pharmaceutical Sciences, University of Toronto, Canada).

Generation of epitope-labeled CaSR-GABA_{B1} and CaSR-GABA_{B2} chimeras

Various constructs were generated in pcDNA3.1(+) using combinations of site-directed mutagenesis polymerase chain reaction (PCR) and restriction digests, DNA purification, and ligations. cDNAs encoding CaSR/GABA_{B1} or CaSR/GABA_{B2} chimeras were synthesized to include: (i) a 5'-end encoding the N-terminus of the WTCaSR (WTCaSR) or CaSR modified by either the FLAG or c-Myc peptides between residues 371 and 372, and (ii) a 3'-end encoding the C-terminus of either GABA_{B1} or GABA_{B2}. Insertions of the FLAG or c-Myc epitopes between residues 371 and 372 were used to permit ELISAs of total and cell surface expression, Western blotting, co-immunoprecipitation, and time-resolved fluorescence (TRF) analysis.

Constructs that were FLAG-tagged or c-Myc-tagged between CaSR residues 371 and 372

CaSR constructs that were labeled with FLAG epitopes between residues 371 and 372 are denoted “*” for: (i) the full-length CaSR, CaSR*; (ii) various CaSR-B1 chimeras, CaSR*₈₆₅-B1, CaSR*₈₇₅-B1, CaSR*₈₉₀-B1, and CaSR*₉₀₈-B1; (iii) various CaSR C-terminal truncation controls, CaSR*_{866X}, CaSR*_{876X}, CaSR*_{891X}, and CaSR*_{909X}; and (iv) the CaSR-B2 chimera, CaSR*₉₀₈-B2. CaSR constructs that were labeled with c-Myc epitopes between residues 371 and 372 are denoted CaSR† (full-length), and for the CaSR-B2 chimera, CaSR†₉₀₈-B2. In all cases either CaSR* or CaSR† was used as the cDNA template to generate chimeras.

CaSR-B1 chimeras

CaSR₉₀₈-B1

GABA_{B1} cDNA encoding C-terminal residues 854–960 (Protein database AAD22194.2) and a stop codon was amplified by PCR with primers to introduce a 5'*Bam* HI and a 3'*Xba* I restriction sites for ligation (Table S1). The PCR product encoding the C-terminus of GABA_{B1} was then digested with *Bam* HI and *Xba* I and ligated into the pcDNA3.1(+)-CaSR backbone that had been predigested with *Bam* HI and *Xba* I to remove residues 909–1078 of the human CaSR C-terminus; ie, to leave CaSR₁₋₉₀₈. Upon ligation of the C-terminus of GABA_{B1} into this construct, the chimera CaSR₉₀₈-B1 was generated. pcDNA3.1 containing CaSR₉₀₈-B1 was used to generate other CaSR-B1 chimeras in which the CaSR C-terminus was further truncated.

CaSR₈₉₀-B1, CaSR₈₇₅-B1 and CaSR₈₆₅-B1

CaSR₉₀₈-B1 was digested with *Kpn* I and *Bam* HI to excise the CaSR fragment, leaving a pcDNA3.1(+) backbone that retained the GABA_{B1} C-terminus in the Multiple Cloning Site (MCS). Using the WTCaSR as the template, successive truncations of the CaSR C-terminus were made by PCR to generate *CaSR*₈₉₀-B1, *CaSR*₈₇₅-B1, and *CaSR*₈₆₅-B1. In particular, a forward primer with a 5'*Kpn* I site was used in conjunction with three distinct reverse primers encoding each of the required CaSR truncations and a 3'*Bam*HI site (Table S1).

CaSR*₈₇₅-B1(ASAR)

Site-directed mutagenesis of GABA_{B1} C-terminal residues 922–925 (from *RSRR* to *ASAR*) in *CaSR**₈₇₅-*B1* was performed using the Quikchange II site-directed mutagenesis protocol with the *PfuUltra* II Fusion HS DNA polymerase (Agilent Technologies, Santa Clara, CA, USA). Pairs of complementary primers that contained the desired mutations were used (Table S2). Following PCR amplification (18 cycles) products were digested with *Dpn* I to degrade the parent DNA prior to transformation into DH5 α *Escherichia coli* cells. This construct is referred to as CaSR*₈₇₅-B1_{ASAR}.

CaSR-B2 chimeras

CaSR₉₀₈-B2

The GABA_{B2} C-terminus encoding residues 760–941 (Protein database NP_005449.5) and a stop codon was amplified by PCR with primers introducing a 5' *Bam* HI site and a 3' *Xba* I site (Table S1). The PCR product was digested with *Bam* HI and *Xba* I and ligated into the pcDNA3.1(+)-CaSR₉₀₈ backbone.

Control CaSR truncated constructs

The following CaSR truncation controls were used: CaSR_{866X}, CaSR_{876X}, CaSR_{891X}, and CaSR_{909X}. Briefly, pcDNA3.1(+) containing WTCaSR between *Kpn* I and *Xba* I restriction sites in the MCS was used as the template in PCR reactions. A common forward primer containing a *Kpn* I site at its 5'-end hybridized to the 5'-end of the WTCaSR and distinct reverse primers containing 3' *Xba* I sites hybridized to the sites of truncation (Table S1). PCR products were digested with *Kpn* I and *Xba* I and ligated into predigested pcDNA3.1(+).

Mutations of the VFT domains or HH-intraloop domains in CaSR₈₇₅-B1 and CaSR₉₀₈-B2

Selected mutations known to impair the function of either the VFT domain (G143E, R185Q) or HH bundles (F706A, L797A) were generated by either site-directed mutagenesis or by digestion of selected DNA fragments using specific restriction enzymes followed by ligation (Table S2). Mutations were introduced either alone or in combination into the WTCaSR, CaSR₈₇₅-B1, or CaSR₉₀₈-B2 backbone, with and without FLAG tags between residues 371 and 372. CaSR mutants F706A (iL-2) and L797A (iL-3) were as described.⁽³⁴⁾

Quantitation of cell total and surface expression of receptor constructs by ELISA

HEK-293 cells were cultured in six-well plates and transiently transfected for 24 hours with WT or mutant forms of CaSR*, CaSR* truncation controls, CaSR*-B1 or CaSR*-B2 chimeras (as described above, * denotes constructs FLAG-tagged between CaSR residues 371 and 372) then harvested and transferred to poly-D-lysine coated 96-well plates for a further 24 hours prior to the assays of total and surface expression. The cells were then washed with TBS-T (0.05M Tris, 0.15M NaCl, 0.05% [vol/vol] Tween-20, pH 7.4) and fixed on ice for 15 minutes with (i) for surface expression, paraformaldehyde 4% (wt/vol) in PBS (137 mM NaCl, 2.7 mM KCl, 10 mM Na₂HPO₄, 1.8 mM KH₂PO₄, pH 7.4) or (ii) for total expression, 100% methanol.⁽³⁷⁾

All subsequent steps were performed at RT. Following fixation, the cells were washed once with TBS-T, blocked with 1% (wt/vol)

skim milk in TBS-T for 1 hour, then incubated with a monoclonal anti-FLAG M2 horseradish peroxidase (HRP)-conjugated antibody (Sigma-Aldrich, St. Louis, MO, USA; #A8592, Australia) diluted 1:5000 in TBS-T for 1 hour. The cells were then washed three times with control TBS-T and incubated with HRP substrate solution containing 3, 3',5, 5' tetramethylbenzidine (Sigma Aldrich, North Ryde, NSW, Australia; #T0440) in the dark for 12 minutes. The substrate reaction was stopped with one volume of 1M HCl. Reaction supernatants were transferred to a new plate and absorbance at 450 nm (A_{450}) was measured using a Wallac EnVision 2103 multilabel counter (EnVision Manager 1.08 software; Perkin Elmer, Waltham, MA, USA). Vector-only background results were subtracted and the results were normalized to total WTCaSR expression defined as 100%.

Microfluorometry method for Ca²⁺_i mobilization

Microfluorometry was performed to measure changes in Ca²⁺_i as described.^(38,39) Briefly, HEK-293 cells were cultured on 15-mm sterile glass coverslips in 24-well plates. Transfected cells were washed once with prewarmed (37°C) Physiological Saline Solution (PSS; 125mM NaCl, 4mM KCl, 20mM HEPES, 0.1% D-Glucose, 0.5mM CaCl₂, 1mM MgCl₂, 0.8mM Na₂HPO₄, pH 7.45 adjusted with NaOH) then incubated in Loading Solution (PSS supplemented with 1 mg/mL bovine serum albumin) containing 5 μ M Fura 2-acetoxymethyl ester (Fura 2-AM) in the dark for 90–120 minutes at 37°C. The cells were then washed with prewarmed PSS and stored in Loading Solution (minus Fura-2 AM) until required.

Coverslips to which fura2-loaded transfected HEK-293 cells adhered were then transferred into a perfusion chamber in the light path of a Zeiss Axiovert 200 M fluorescence microscope (\times 63 objective; Carl Zeiss Microscopy, Inc., Dublin, CA, USA). The cells were perfused with phosphate-free PSS adjusted to contain various extracellular Ca²⁺ (Ca²⁺_o) concentrations (0.5–30mM) as required. Fura-2 loaded cells were excited at alternating wavelengths of 340 nm and 380 nm at 0.5-second intervals using a Lambda DG-4 150 W Xenon light source (Sutter Instrument Company, Novato, CA, USA) and emission images were collected at 510 nm using an AxioCam H5m digital camera (Zeiss). Changes in Ca²⁺_i were detected and saved as changes in F₃₄₀/F₃₈₀ excitation ratios using Stallion SB.4.1.0 PC software (Intelligent Imaging Solutions, Denver, CO, USA). For the generation of Ca²⁺_o concentration-response curves, Ca²⁺_i responses from single cells were integrated to provide results in the form of integrated fluorescence response units (IFRUs) that were corrected for the baseline control (0.5mM Ca²⁺_o), as described.⁽³⁹⁾ In general, HEK-293 cells were transfected with non-tagged constructs for functional analyses. One exception was the FLAG-tagged construct CaSR*(F706A)₈₇₅-B1. The insertion site of the FLAG peptide (CaSR residues 371 and 372) is functionally inert.⁽⁴⁰⁾

IP₁ assay in HEK-293 cell suspensions

These assays were performed in a manner similar to that described.⁽³⁴⁾ Briefly, HEK-293 cells were subcultured into six-well plates and culture media were replaced 24 hours posttransfection. After a further 24 hours, cells were detached using trypsin-EDTA (1 mL) for 3 minutes at 37°C, and tryptic activity was quenched by the addition of 4 mL culture medium (10% FBS). Following detachment, cells were harvested by centrifugation (410g, 2 minutes), washed once with 5 mL phosphate-free

PSS, re-centrifuged, and then resuspended in 1 mL phosphate-free PSS. An aliquot of cells was then counted in a Countess electronic hemocytometer (Invitrogen).

After adjusting the cell density to $\sim 10,000$ cells/well, 7- μ L lots of cell suspension were transferred to the wells of a 384-well plate (Perkin Elmer OptiPlate; Perkin-Elmer) and preincubated for 5 minutes at 37°C. Following preincubation, 7- μ L lots of various Ca²⁺-containing stock solutions in PSS were added to achieve final concentrations in the range 0.5–20mM and plates were then incubated for 30 minutes at 37°C. To estimate IP₁ production in cell lysates, Cisbio IP₁ HTRF kits (Perkin-Elmer) were used according to the manufacturer's instructions and plates were read following 1-hour incubations at room temperature in a Tecan Infinite M1000 Pro TRF plate reader (Tecan Trading AG, Männedorf, Switzerland).

Immunoprecipitation of FLAG-labeled proteins and detection of co-immunoprecipitated c-Myc-labeled proteins

HEK-293 cells were subcultured in six-well plates and transfected for 48 hours as required. Transfected cells were washed twice with ice-cold PBS (137mM NaCl, 2.7mM KCl, 10mM Na₂PO₄, 1.8mM KH₂PO₄, pH 7.4) then detached and lysed with 0.5 mL radioimmunoprecipitation assay (RIPA) buffer (150mM NaCl, 1% NP-40, 0.1% sodium dodecylsulfate [SDS], 1%, sodium deoxycholate, 25mM Tris-HCl, pH 7.6). Lysate samples were passed through 21G needles 10 times to facilitate disruption and detergent solubilization, then incubated on ice for 10 min. Samples were then centrifuged at 12,000g for 10 minutes at 4°C and the supernatants (0.05 mL) were then collected and added to 0.05 mL samples of anti-FLAG M2 Affinity gel (Merck, Sigma-Aldrich, North Ryde, NSW, Australia; #A2220) that had been washed with Equilibration Buffer (50mM Tris-HCl, 150mM NaCl, 0.5% Triton X-100, pH 7.6) three times at RT. Suspensions of cell lysates and gel beads were incubated overnight by vertical rotation at 4°C and the beads were then pelleted in a microfuge. The supernatants were discarded and the beads were washed five times with Equilibration Buffer. Proteins that had been immunoprecipitated on anti-FLAG M2 Affinity gel were then eluted using 30 μ L Pull-down Buffer; ie, Equilibration Buffer containing soluble 150 μ g/mL 3 \times FLAG peptide (Sigma-Aldrich; #F4799) by vertical rotation for 30 minutes at 4°C followed by centrifugation (microfuge, 10 minutes) and the supernatants were collected for further analysis by sodium dodecyl sulfate–polyacrylamide gel electrophoresis (SDS-PAGE) and Western blotting.

For the detection of co-immunoprecipitated c-Myc containing proteins, SDS-PAGE of immunoprecipitated proteins was performed using a 7.5% polyacrylamide resolving and a 4% stacking gel and the proteins then underwent electrotransfer to nitrocellulose membranes as described.⁽⁴¹⁾ Membranes were blocked with solutions containing 5% milk and incubated overnight with anti-c-Myc Epitope Antibody (HRP-conjugated; 1:500 dilution; Thermo Fisher Scientific, Waltham, MA, USA; #ab1326). Following incubation with HRP substrate, images of the membranes were captured using a BioRad Chemidoc system (Bio-Rad Laboratories, Hercules, CA, USA).

Time-resolved Fluorescence

For Time-resolved Fluorescence (TRF), HEK-293 cells were subcultured in six-well plates and transfected or co-transfected with FLAG and c-Myc labeled CaSR₈₇₅-B1 and/or CaSR₉₀₈-B2 receptor constructs as required. Briefly, HEK-293 cells were cultured in

1.5 mL per well of complete medium (DMEM/10% FBS/0.05% penicillin–streptomycin). For transfection, DNA amounts of 0.35 μ g per sample per well or 0.15 μ g per sample per well were used and added in volumes of 0.5–3 μ L to 150 μ L lots of antibiotic-free, FBS-free DMEM followed by 4.5- μ L lots of XtremeGENE HP (Sigma-Aldrich; #6366244001). The suspensions were allowed to stand at room temperature in a biosafety cabinet for 15 minutes prior to addition to the wells. The plates were then transferred to a CO₂ incubator at 37°C.

Following transfection for 48 hours, the media bathing the cells attached to the bottoms of the wells of six-well plates were removed and replaced by 0.4-mL volumes of Trypsin (0.25%)-EDTA (Gibco-Thermo Fisher-Scientific; #25200056). Following incubation for 2 minutes at 37°C, 1.0-mL volumes of complete medium were added to the wells to prevent further tryptic action, and the layer of cells was gently removed from the bottom of each well by repetitive irrigation using a 1.0-mL pipette. The detached cells were transferred to 10-mL centrifuge tubes and sedimented (Eppendorf 5810 centrifuge; A-4-81 rotor, 314g, 2 minutes). The supernatants were then discarded and cell pellets were resuspended in 0.5-mL lots of PSS (pH 7.4) containing 1.0mM CaCl₂ and 2 mg/mL bovine serum albumin (Sigma-Aldrich; A7906). This solution is henceforth referred to as TRF-PSS. After counting (Invitrogen Countess; cell count range observed 2.5–5 $\times 10^6$ cells/mL), 40,000 cells (transfected with either pcDNA3.1, or CaSR^{*}₈₇₅-B1, or CaSR[†]₉₀₈-B2, or both CaSR^{*}₈₇₅-B1 and CaSR[†]₉₀₈-B2) were transferred into 0.5-mL microfuge tubes for antibody incubations, which were performed in TRF-PSS (pH 7.4). The incubations (total volumes 30 μ L) contained, in addition to 40,000 cells, either no antibodies, or 5 μ L of freshly diluted Anti-FLAG: Tb cryptate (5- μ L aliquots of concentrated stock plus 140- μ L lots of TRF-PSS) or 5 μ L of freshly diluted Anti-Myc:XL665 (5- μ L aliquots of concentrated stock plus 140- μ L lots of TRF-PSS) or 5 μ L of each of these two antibodies. In some experiments, Anti-Myc:XL665 was replaced by Anti-Myc:d2 (2- μ L aliquots of concentrated stock plus 140- μ L lots of TRF-PSS). Stocks of all three antibodies (Cisbio; #61FG2TLA; #61MYCXLA; #61MYCDAF, respectively) were made up in water according to the manufacturer's instructions (0.25 mL, 0.25 mL, and 0.08 mL, respectively) and stored in aliquots (5 μ L, 5 μ L, and 2 μ L, respectively) at –30°C. Incubations (23°C) were started by the addition of cells and the microfuge tubes were then transferred to the surface of a horizontal rocker (10 cycles per minute). After 90 minutes, the tubes (batches of 24) were transferred to the rotor of a Heraeus Biofuge Fresco benchtop centrifuge (Thermo-Fisher, Macquarie Park, NSW Australia), using 1.5-mL microfuge tubes as adapters, and the cells were sedimented (6100g for 3 minutes). To remove excess soluble antibodies and to reduce nonspecific binding to the cells, the tubes were transferred to racks that held them tightly in position and opened. The racks were then inverted and the supernatants were discarded by repetitive firm striking onto layers of absorbent paper. After returning the tubes to the upright position, the cell pellets were resuspended in 60- μ L lots of TRF-PSS, washed by repeat centrifugation, and returned to the racks for repeat inversion and discarding of supernatants. The samples were finally resuspended in 40- μ L lots of TRF-PSS without bovine serum albumin (BSA) and transferred to individual wells of 384-well styrene white Optiplates (Perkin Elmer; #6007290) for counting according to a TRF protocol.

Plates were read using a Tecan infinite M1000 plate reader according to a Cisbio-derived TRF protocol with excitation (100 flashes at 100 Hz) and emission capture performed in two

separate sequences: (i) 340 nm (bandwidth 20 nm) and emission 620 nm (bandwidth 10 nm); and (ii) 340 nm (20 nm bandwidth) and emission 665 nm (10 nm bandwidth). TRF data were collected for intervals of 0.5 ms with lag times following each pulse of excitation of 0.06 ms. Reductions in F620 emission from Tb-cryptate in the presence of XL665 were used to assess Förster Resonance Energy Transfer (FRET). The effectiveness of 340-nm excited Tb-cryptate emission (at 620 nm) in exciting XL665 was assessed by the emission responses observed at 665 nm.

Fluorescence imaging of cells

HEK-293 cells were seeded into poly-D-lysine coated (50 µg/ml) iBidi eight-chamber slides at a density of 100,000 cells per chamber and allowed to adhere for 4 hours. Cells were transfected with 0.2 or 0.4 µg DNA (0.2 µg CaSR*₈₇₅-B1, or 0.2 µg CaSR*₈₇₅-B1+ 0.2 µg CaSR₉₀₈-B2) using a 1:4 ratio of DNA:lipofectamine-2000 (in a final volume of 50 µL Optimum).

The following day, DMEM was replaced with serum-free DMEM containing 0.1mM Ca²⁺. After 24 hours, cells were washed with PBS and then fixed using 4% paraformaldehyde for 10 minutes on ice, washed 3× with PBS/Azide (0.1% NaN₃), and then incubated in blocking buffer (5% horse serum and 0.1% saponin in PBS/Azide) for 1 hour at RT.

Anti-FLAG M2 monoclonal antibody (Sigma-Aldrich) was diluted to 1 µg/mL in blocking buffer and incubated with cells for 4 hours at 4°C. Cells were washed 3× with PBS/Azide for 10 minutes each and then incubated for 1 hour with goat anti-mouse Alexa Fluor 647 Plus (Invitrogen/Thermo Fisher Scientific) diluted 1:500 in PBS/Azide at RT. The cells were washed 1× with PBS/Azide, incubated with DAPI (1:1000 in PBS/Azide) for 5 minutes, washed 2× with PBS Azide and stored at 4°C overnight prior to confocal imaging. Imaging was performed using a Leica SP8 inverted scanning confocal microscope (Leica, Wetzlar, Germany) and data were analyzed with ImageJ software (NIH, Bethesda, MD, USA; <https://imagej.nih.gov/ij/>).

Curve fitting and statistical analysis

The results are routinely expressed as mean ± SE (*n*) where *n* is the number of independent experiments. Integrated F₃₄₀/F₃₈₀ ratios from Ca²⁺_i mobilization assays were fitted to the Hill equation:|

$$R = d + (a - d) * C^b / (e^b + C^b) \quad (1)$$

where *R* = receptor response, *a* = maximal response, *b* = Hill coefficient, *C* = agonist concentration, *d* = minimum response, and *e* = half-maximal effective concentration.

Statistical analyses were performed using GraphPad Prism software (GraphPad Software, Inc., La Jolla, CA, USA), with statistical significance accepted at *p* < 0.05. Comparisons between Ca²⁺_o concentration-response curves were performed using pEC₅₀ values (ie, after log transformation) and E_{max} values.

Results

Expression and function of CaSR-GABA_B chimeras and CaSR C-terminal truncation controls

Construct libraries and total and surface expression in transfected HEK-293 cells

The dimer interaction characteristics of the GABA_{B1} and GABA_{B2} C-termini were used to generate CaSR-GABA_B

chimeras capable of forming a heterodimer trafficking system, as described for mGlu receptors.⁽³¹⁾ For the generation of suitable CaSR constructs, we used a WT human CaSR and a variant that had been modified by the insertion of a FLAG epitope tag DYKDDDDK in the receptor's VFT domain, between residues 371 and 372,⁽³⁵⁾ to permit quantitation of total and surface expression by ELISA. Insertion of the FLAG peptide at this site is functionally silent.⁽⁴⁰⁾ Constructs bearing the FLAG peptide are identified by the inclusion of an "*""; eg, CaSR*(WT or mutant); CaSR*(WT or mutant)-B1. The "*" is omitted when referring to constructs in which the FLAG epitope was absent; eg, CaSR(WT or mutant).

The CaSR C-terminus contains elements that modulate receptor expression, trafficking and function.^(42,43) To determine the optimal position of the GABA_{B1} C-terminus so that the CaSR-GABA_{B1} chimera would be retained intracellularly with impacts on cell surface expression and receptor function, we generated a library of FLAG-tagged CaSR-GABA_{B1} chimeras in which the CaSR C-terminus was truncated after residues 908, 890, 875, or 865, and the GABA_{B1} C-terminus (residues 854–960) was appended in-frame (Fig. 1A). A control library of FLAG-tagged truncated CaSRs, in which stop codons were introduced at positions 909, 891, 876, or 866, was also generated. To facilitate the formation of trafficking competent, and potentially functional, heterodimers with the various CaSR-B1 constructs, a further receptor construct was made in which the GABA_{B2} C-terminus (residues 760–941) was appended after CaSR residue 908 (Fig. 2). To quantify total and surface expression of CaSR₉₀₈-B2, a FLAG-tagged variant, CaSR*₉₀₈-B2, was generated. In studies of its impact on CaSR*₈₇₅-B1 expression, however, untagged CaSR₉₀₈-B2 was used.

Total and cell surface expressions of FLAG-tagged WTCaSR and chimeras were analyzed in transfected HEK-293 cells using anti-FLAG antibody-based ELISAs and the results were normalized to WTCaSR total expression (Table 1). With respect to total expression, no significant differences were observed between the WTCaSR and any of the CaSR-B1 chimeras or CaSR truncation controls tested (Table 1). However, substantial differences in surface expression were observed between the WTCaSR and various chimeras and mutants.

For the WTCaSR surface expression was 68% ± 3% of total expression (*n* = 18; Table 1) and CaSR truncation mutants 909X and 891X exhibited increased levels of surface expression to 92% ± 9% and 101% ± 8%, respectively, of WT total expression (*p* = 0.01 and *p* = 0.0012; *n* = 3 in each case). Surface expression levels for CaSR truncation mutants 876X and 866X, however, were not significantly different from the WT control (*p* > 0.1; *n* = 3 in each case). In the cases of all four CaSR-B1 chimeras assessed, however, we observed substantial reductions in cell surface expression to around 30%–40% irrespective of the site in the CaSR C-terminus to which the GABA_{B1} C-terminus was appended (Table 1). Thus, trafficking of CaSR-B1 chimeras to the plasma membrane was restricted by the ER retention motif in the GABA_{B1} C-terminus.

We next investigated the subcellular localization of the WTCaSR and CaSR-B1 chimeras using an Alexa Fluor 647-tagged anti-FLAG antibody. Fluorescence microscopy of labeled HEK-293 cells transfected with WTCaSR or one of the CaSR-B1 chimeras demonstrated that whereas the WTCaSR localized to the periphery of cells (ie, to the plasma membrane and/or just deep to it), CaSR-GABA_{B1} chimeras were more diffusely distributed in the cytoplasm and perinuclear region (Fig. 1B).

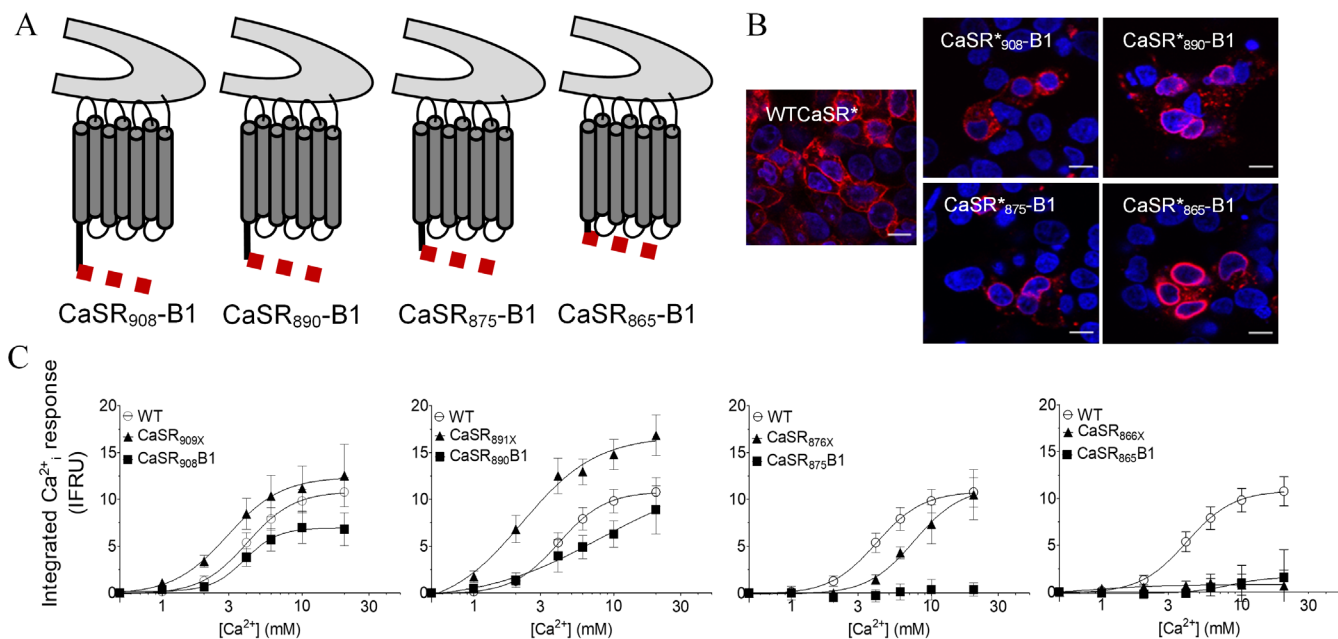


Fig. 1. Library of CaSR-GABAB1 chimeras. (A) Schematic representations of CaSR-GABAB1 chimeras, in which the GABAB1 C-terminus (residues 854–960; red), is appended after CaSR residue 908, 890, 875, or 865; four control CaSR constructs with stop codons at 909, 891, 876, or 866 are not shown. (B) Fluorescence microscopy of HEK-293 cells transfected with WTCaSR or CaSR-GABAB1 chimeras. Cells were labeled with Alexa-Fluor 647 Plus goat anti-mouse antibody directed against M2 anti-FLAG antibody for FLAG-tagged receptors, and nuclei were stained with DAPI ($n = 3$). Scale bars = 10 μm . (C) Ca^{2+}_o -stimulated Ca^{2+}_i mobilization in Fura2-loaded HEK-293 cells transfected with CaSR-GABAB1 chimeras and CaSR truncation mutants and corrected for responses in Fura2-loaded HEK-293 cells transfected with pcDNA3.1. Integrated data were fitted to Equation (1) ($n = 3$ –8).

Functional characterization of HEK-293 cells transfected singly with CaSR-GABA(B1) chimeras or CaSR truncation mutants in assays of Ca^{2+}_o -induced Ca^{2+}_i mobilization

We assessed the function of the WTCaSR, CaSR truncation mutants and CaSR-GABA_B chimeras by Ca^{2+}_o -induced Ca^{2+}_i mobilization in HEK-293 cells that had been transfected for

48 hours then loaded with Fura-2 AM, and exposed to stepwise increments in Ca^{2+}_o in a live cell imaging apparatus (Fig. 1C). HEK-293 cells transfected with the WTCaSR exhibited Ca^{2+}_o -dependent Ca^{2+}_i mobilization with an half maximal effective concentration (EC_{50}) for Ca^{2+}_o of $4.0 \pm 0.1 \text{ mM}$ and a maximal response of 11 ± 0.1 Integrated Fluorescence Ratio Units (IFRU; $n = 8$). Consistent with enhanced membrane expression see previous Results section, the truncation mutants CaSR_{909X} and CaSR_{891X} exhibited increased maximum effect (E_{max}) values. The effect was pronounced for CaSR_{891X}, whose E_{max} value increased to 16.8 ± 2.2 IFRU ($p = 0.007$; $n = 4$). In the case of the CaSR truncation mutant CaSR_{876X}, we observed no change in E_{max} compared to WT but an increase in EC_{50} for Ca^{2+}_o to $7.5 \pm 0.5 \text{ mM}$ ($p < 0.001$; $n = 4$). Finally, and despite levels of total and surface expression that were comparable to WT (Table 1), CaSR_{866X} did not support Ca^{2+}_o -dependent Ca^{2+}_i signaling, as reported previously.^(34,42)

We next investigated the function of CaSR-B1 chimeras. Appending the GABA_{B1} C-terminus lowered the E_{max} values by 30%–40% when compared to the WTCaSR to 6.9 ± 0.2 IFRU for CaSR₉₀₈-B1 and 8.9 ± 2.6 IFRU for CaSR₈₉₀-B1. In the case of CaSR₈₇₅-B1, however, appending the GABA_{B1} C-terminus abolished Ca^{2+}_o -induced Ca^{2+}_i mobilization at concentrations up to 20mM (Fig. 1C). Similarly, and consistent with the behavior of its truncation mutant control (CaSR_{866X}), HEK-293 cells transfected with CaSR₈₆₅-B1 did not support Ca^{2+}_o -induced Ca^{2+}_i mobilization (Fig. 1C).

Taken together, the functional results for the CaSR-B1 chimeras and their truncation controls demonstrated that only one CaSR-B1 construct, CaSR₈₇₅-B1, exhibited markedly impaired

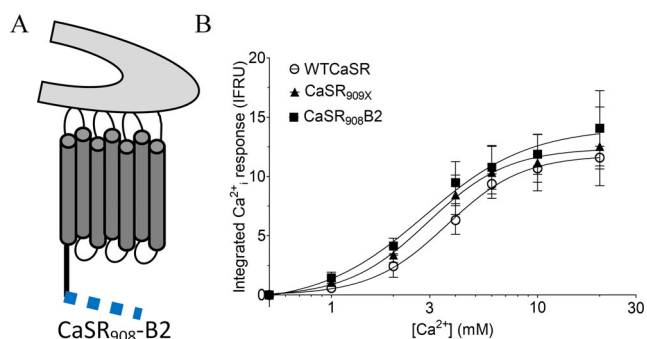


Fig. 2. CaSR908-B2 expression and function. (A) Schematic representation of chimera composed of CaSR residues 1–908 and GABAB2 residues 760–941. (B) Ca^{2+}_o -stimulated Ca^{2+}_i mobilization responses in Fura2-loaded HEK-293 cells transfected with WTCaSR, the CaSR908-B2 chimera, or the CaSR truncation mutant control CaSR909X. Integrated data were fitted to Equation (1) ($n = 4$ –6). The results were corrected for responses in Fura2-loaded HEK-293 cells transfected with pcDNA3.1.

Table 1. Total Expression and Surface Expression of Various FLAG Epitope-Tagged CaSR Constructs in Transfected HEK-293 Cells

CaSR construct (n)	Surface expression (% total WT-CaSR)	Total expression (% total WT-CaSR)
WT-CaSR* (18)	68.3 ± 3.2 ¹⁻⁹	101 ± 1.0
CaSR* ₉₀₈ -B1 (6)	31.8 ± 7.0 ^{1,10}	109 ± 5.1
CaSR* ₈₉₀ -B1 (10)	43.8 ± 7.8 ^{2,11}	100 ± 4.6
CaSR* ₈₇₅ -B1 (4)	40.4 ± 7.8 ^{3,12}	104 ± 4.0
CaSR* ₈₆₅ -B1 (7)	40.3 ± 7.6 ^{4,13}	96.4 ± 3.6
CaSR* ₉₀₈ -B2 (6)	92.8 ± 3.0 ⁵	100 ± 3.5
CaSR* _{909X} (3)	92.0 ± 8.5 ^{6,10}	108 ± 4.7
CaSR* _{891X} (3)	101 ± 7.8 ^{7,11}	117 ± 5.9
CaSR* _{876X} (3)	82.7 ± 11 ^{8,12}	111 ± 4.2
CaSR* _{866X} (3)	70.5 ± 7.3 ^{9,13}	106 ± 2.2
One-way ANOVA	F = 11.1; p < 0.0001	F = 2.1; p = 0.05 (ns)
Student's post test (*Welch's t used due to difference in variance)	1. p < 0.0001; 2. p = 0.013*; 3. p = 0.0017; 4. p = 0.0005; 5. p = 0.0004; 6. p = 0.012; 7. p = 0.0012; 8. p = 0.13; 9. p = 0.80; 10. p = 0.0013; 11. p = 0.003; 12. p = 0.022; 13. p = 0.046	Not indicated

HEK-293 cells were transfected or co-transfected with various CaSR constructs and then assessed for surface and total expression as described in the Materials and Methods section. The presence of a FLAG epitope in the VFT domain of various CaSR constructs is denoted CaSR*. The total and surface expression were determined for WT-CaSR, various CaSR-B1 chimeras, a CaSR-B2 chimera (CaSR*₉₀₈-B2), and various CaSR truncation controls as shown. As an example, CaSR*₉₀₈-B1 was FLAG epitope labeled and the GABA(B1) C-terminus was appended after CaSR residue S908. The data were normally distributed (Shapiro-Wilk; QQ plot). Two-way ANOVA reported significant differences for *CaSR Construct* (F = 16.8, p < 0.0001), *Type of Expression* (F = 33.0, p < 0.0001), and the *Interaction* (F = 12.6, p < 0.0001). Results of one-way ANOVA and, where indicated, Student's t post tests (selected due to an absence of differences in variance) are shown at bottom. All surface expression and total expression data (means ± SE) are reported as % of WT-CaSR total expression. Superscript numbers in italics designate comparisons between elements in columns.

receptor function, as determined by Ca²⁺_o-induced Ca²⁺_i mobilization, dependent on the presence of the GABA-B1 C-terminus. We used this construct in further studies in which CaSR₈₇₅-B1, and selected mutants derived from it, were co-expressed with a suitable CaSR-B2 chimera with the aim of generating B1-B2 heterodimers that traffic to the cell surface and support Ca²⁺_o-induced Ca²⁺_i mobilization.

Total and surface expression and function of CaSR₉₀₈-B2 when transfected singly in HEK-293 cells

In developing a CaSR-B2 chimera capable of trafficking CaSR₈₇₅-B1 to the cell surface we initially generated CaSR*₉₀₈-B2 (Fig. 2A) and the control truncation CaSR*_{909X}. When transfected into HEK-293 cells, both constructs were efficiently expressed in total and cell surface expression assays (Table 1), and were functionally similar to the WT-CaSR as determined by Ca²⁺_o-induced Ca²⁺_i mobilization (Fig. 2B).

Impact of CaSR₉₀₈-B2 and role of GABA_{B1} ER retention motif on CaSR₈₇₅-B1 trafficking

HEK-293 cells were co-transfected with CaSR*₈₇₅-B1 and either untagged CaSR₉₀₈-B2 or its control CaSR_{909X} to evaluate their impacts on surface expression. CaSR*₈₇₅-B1 was efficiently trafficked to the cell surface by CaSR₉₀₈-B2 but not CaSR_{909X} (Table 2). Due to the success of CaSR₉₀₈-B2 in its intended trafficking role, we did not investigate alternative CaSR-B2 constructs but instead proceeded to an extended analysis of receptor expression and function in HEK-293 cells transfected with CaSR*₈₇₅-B1 in the absence or presence of CaSR₉₀₈-B2. Thus these complementary constructs permitted studies of mutant heterodimers.

We next investigated whether impaired surface expression of CaSR*₈₇₅-B1 was dependent on the GABA_{B1} C-terminal ER

retention peptide *RSRR*, utilizing the mutant CaSR*₈₇₅-B1_{ASAR}, which removes two key basic residues that provide local positive charge. Total protein expressions of all constructs were comparable (Table 2). However, significant differences in surface expression were observed. In these experiments, the ratio of surface to total expression was 83% ± 2.2% (n = 6) for the full-length WT-CaSR and was markedly reduced to 30% ± 2% (n = 6) for CaSR*₈₇₅-B1 as expected (p < 0.001). Interestingly, the mutant CaSR*₈₇₅-B1_{ASAR}, however, exhibited no change in total expression but increased surface expression that was 95% ± 5% (n = 4) of WT-CaSR total expression (Table 2). The results demonstrate that cell surface expression of CaSR*₈₇₅-B1 was selectively rescued in cells co-transfected with CaSR₉₀₈-B2 and that impaired trafficking of CaSR*₈₇₅-B1 in the absence of CaSR₉₀₈-B2 was entirely dependent on the ER retention motif *RSRR* in the GABA_{B1} C-terminus.

Detection of heterodimers in cells co-transfected with CaSR₈₇₅-B1 and CaSR₉₀₈-B2 constructs

TRF assays to detect Förster resonance energy transfer

To investigate whether heterodimer formation was responsible for trafficking of CaSR₈₇₅-B1 to the cell surface by CaSR₉₀₈-B2, we utilized CaSR*₈₇₅-B1 and CaSR†₉₀₈-B2 in a modified TRF assay. CaSR†₉₀₈-B2 was modified from CaSR₉₀₈-B2 by the introduction of the peptide epitope *EQKLISEEDL* derived from the transcription factor c-Myc between residues 371 and 372. After initial optimization, HEK-293 cells were cultured in six-well plates and transfected with either pcDNA3.1, CaSR*₈₇₅-B1, or CaSR†₉₀₈-B2 individually or CaSR*₈₇₅-B1 and CaSR†₉₀₈-B2. After 48 hours, intact cells were collected by limited trypsin digestion and labeled in triplicate incubations with either: no antibodies; anti-FLAG: Tb³⁺-cryptate (donor fluorophore; emission max 620 nm); or anti-c-Myc: XL-665 (acceptor fluorophore; emission max

Table 2. Trafficking of CaSR*₈₇₅-B1 to the Cell Surface by CaSR₉₀₈-B2 and Role of GABA(B1) C-Terminal Peptide RSRR in ER Retention

CaSR construct (n)	Surface expression (% total WT-CaSR)	Total expression (% total WT-CaSR)
WT-CaSR* (6)	82.5 ± 2.3 ^{1,2}	102.2 ± 1.2 ¹⁻⁴
CaSR* ₈₇₅ -B1 (6)	30.9 ± 2.0 ^{1,3-5}	97.4 ± 2.2 ^{1,5,6,7}
CaSR* ₈₇₅ -B1(ASAR) (4)	94.5 ± 5.0 ^{2,3}	103.8 ± 3.2 ^{2,5}
CaSR* ₈₇₅ -B1 and CaSR ₉₀₈ -B2 (4)	58.0 ± 5.6 ⁴	89.8 ± 7.9 ^{3,6}
CaSR* ₈₇₅ -B1 and CaSR _{909X} (3)	24.7 ± 4.0 ⁵	84.1 ± 6.0 ^{4,7}
Welch's post test	1. <i>p</i> < 0.0001; 2. <i>p</i> = 0.09; 3. <i>p</i> = 0.0003; 4. <i>p</i> = 0.01; 5. <i>p</i> = 0.26	1. <i>p</i> = 0.09; 2. <i>p</i> = 0.66; 3. <i>p</i> = 0.22; 4. <i>p</i> = 0.09; 5. <i>p</i> = 0.15; 6. <i>p</i> = 0.42; 7. <i>p</i> = 0.15

HEK-293 cells were transfected or co-transfected with various CaSR constructs and then assessed for surface and total expression as described in the Materials and Methods section. CaSR constructs, whose expression was quantified were labeled with a FLAG peptide epitope in the VFT domain and are denoted as CaSR*. The impacts of unlabelled CaSR₉₀₈-B2 and of mutating an RSRR peptide in the C-terminus of GABA_{B1} were determined. The data were normally distributed (Shapiro-Wilk; QQ plot). 2-way ANOVA reported significant differences for *CaSR Construct* ($F = 50.2, p < 0.0001$), *Type of Expression* ($F = 218, p < 0.0001$), and the *Interaction* ($F = 20.6, p < 0.0001$). All surface expression and total expression data (means ± SE) are reported as % of WT-CaSR total expression. Surface expression of CaSR*₈₇₅-B1 was markedly impaired as predicted from the ER retention properties of the GABA_{B1} C-terminus. This was overcome either by trafficking with CaSR₉₀₈-B2, or in the mutant CaSR*₈₇₅-B1(ASAR), but not by co-transfection of the control construct CaSR_{909X}. Superscript numbers in italics designate comparisons between elements in columns.

665 nm); or both anti-FLAG:Tb³⁺-cryptate and anti-c-Myc:XL665. Cell samples were then sedimented and the supernatants were discarded. They were then washed by centrifugation, resuspended, and transferred to individual wells of a 384-well white Optiwell plate for TRF. Förster resonance energy transfer (FRET) in putative CaSR*₈₇₅-B1:CaSR[†]₉₀₈-B2 heterodimers; ie, in multiple restricted locations in the total cell populations was assessed by reductions in fluorescence emission at 620 nm (F620) from Tb-cryptate in the presence of XL665. The effectiveness of 340 nm-excited Tb-cryptate emission at 620 nm in exciting XL665 in anti-Myc-labeled CaSR[†]₉₀₈-B2 receptor subunits was assessed by emission responses at 665 nm.

TRF data based on fluorescence emissions at 620 nm and 665 nm (respectively, F620 and F665) were obtained in three experiments using 0.35 µg per sample per well and in five experiments using 0.15 µg per sample per well. Because similar TRF results were obtained in all eight experiments (with each experimental condition performed in triplicate; ie, 24 observations in total) we combined the data for both statistical evaluation and presentation (Fig. 3A; Table 3).

TRF results from cells transfected with pcDNA3.1, CaSR*₈₇₅-B1 alone or CaSR[†]₉₀₈-B2 alone

As expected, in cells transfected with pcDNA3.1, after incubation and washing, we observed very low TRF levels at both F620 and F665, regardless of whether the cells were incubated with no antibodies, anti-FLAG:Tb-cryptate alone, anti-Myc:XL665 alone, or with both antibodies. In cells transfected with CaSR*₈₇₅-B1 alone and incubated with anti-FLAG:Tb-cryptate, however, we observed a moderate increase in TRF level at F620 to around 10% of the maximum F620 values observed, consistent with limited CaSR*₈₇₅-B1 surface expression and anti-FLAG:Tb-cryptate binding, but no increase at F665 (Fig. 3A, Table 3). As expected, similar TRF responses at F620 (moderate increase) and F665 (no change from baseline) were observed from cells transfected with CaSR*₈₇₅-B1 alone when incubated in the presence of both anti-FLAG:Tb-cryptate and anti-Myc:XL665, consistent with a failure of anti-Myc:XL665 binding in the absence of CaSR[†]₉₀₈-B2. In cells transfected with CaSR[†]₉₀₈-B2 alone, however, only baseline TRF levels were observed in response to 340 nm excitation at

both F620 and F665, due to the absence of anti-FLAG:Tb-cryptate binding.

TRF results from cells co-transfected with both CaSR*₈₇₅-B1 and CaSR[†]₉₀₈-B2

In cells co-transfected with both CaSR*₈₇₅-B1 and CaSR[†]₉₀₈-B2, we observed a robust TRF signal at F620 in the presence, but not the absence, of anti-FLAG:Tb-cryptate that was significantly reduced by around 15% when cells were co-incubated with anti-Myc:XL665 (Fig. 3A; Table 3; Kruskal-Wallis for co-transfected cells under all four conditions, K-statistic = 74.2, *p* < 0.0001; Mann-Whitney post-test for incubation with both antibodies versus anti-FLAG:Tb-cryptate alone, *p* = 0.003). This observation supports the conclusion that in the presence of the acceptor fluorophore in antibody-bound heterodimeric complexes, donor emission was reduced via (non-radiative) FRET; ie, it supports the existence of heterodimers composed of CaSR*₈₇₅-B1 and CaSR[†]₉₀₈-B2.

Further evidence of CaSR[†]₉₀₈-B2-dependent chaperoning of CaSR*₈₇₅-B1 was also obtained. Thus, the F620 signal arising from anti-FLAG:Tb-cryptate labeling of CaSR*₈₇₅-B1 was markedly increased in co-transfected cells when compared with cells that were transfected with CaSR*₈₇₅-B1 alone (Mann-Whitney post-test for comparison of co-transfected cells versus cells transfected with CaSR*₈₇₅-B1 alone, *p* < 0.0001; Table 3). The corresponding TRF signal at F665 was modest (around 5%–10% of the observed maximum) in co-transfected cells incubated with anti-FLAG:Tb-cryptate alone but robust to 100% of the observed maximum in cells co-incubated with both anti-FLAG:Tb-cryptate and anti-Myc:XL665, indicative of radiative as well as non-radiative energy transfer from anti-FLAG:Tb-cryptate labeled CaSR*₈₇₅-B1 receptor subunits to anti-Myc:XL665 labeled CaSR[†]₉₀₈-B2 receptor subunits (Fig. 3A; Table 3).

Similar results were obtained in a further three experiments performed using DNA amounts of 0.15 µg per sample per well and anti-Myc labeled with the d2 fluorophore rather than XL665 (not shown).

Immunoprecipitation analyses

To confirm that co-expression of CaSR₉₀₈-B2 with CaSR₈₇₅-B1 facilitated the formation of heterodimers, immunoprecipitation

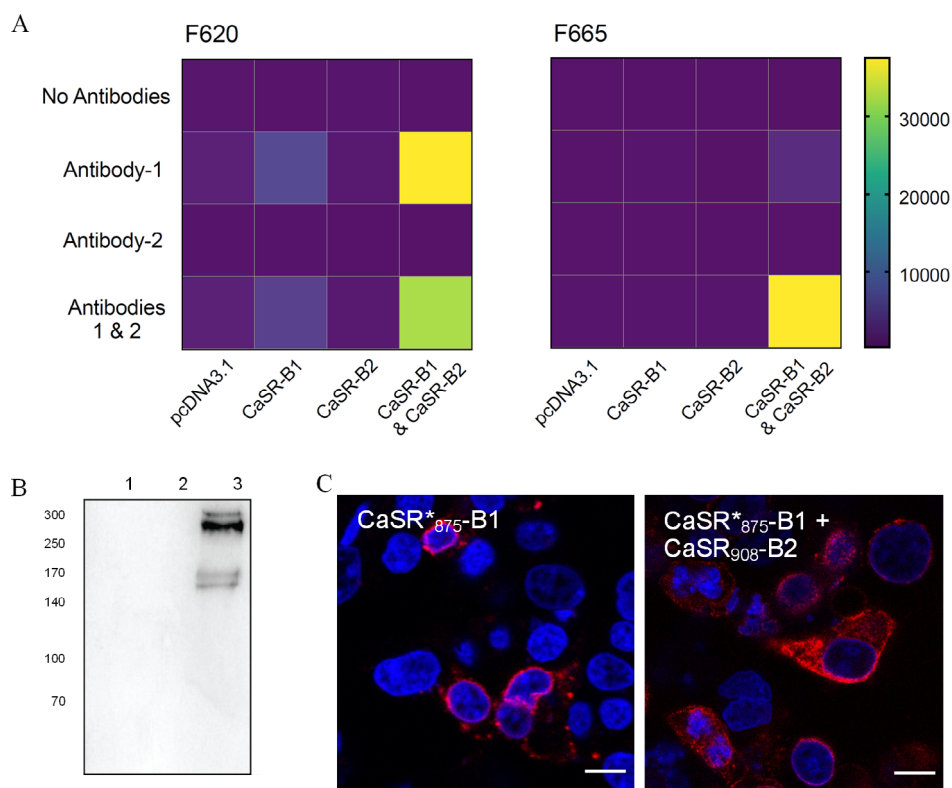


Fig. 3. Evidence that co-expressed CaSR875-B1 and CaSR908-B2 receptor constructs form heterodimers. (A) TRF analysis of HEK-293 cells transfected with various constructs, including pcDNA3.1, CaSR^{*}875-B1 alone, CaSR[†]908-B2 alone, or both chimeras together. Transfected cells were labeled with either (i) no antibodies, or (ii) anti-FLAG:Tb cryptate, which binds selectively to CaSR^{*}875-B1; or (iii) anti-Myc:XL665, which binds selectively to CaSR[†]908-B2; or (iv) both anti-FLAG:Tb cryptate and anti-Myc:XL665. Cell samples were then washed by centrifugation to remove the bulk medium and reduce nonspecific binding as described in Materials and Methods. After resuspension, cell samples were loaded into 384-well Optiplates and analyzed using a TRF protocol in two separate periods in which excitation pulse sequences were delivered at 340 nm in both cases and in which emitted light was collected separately at 620 nm and 665 nm. The heat map summarizes the findings for all four constructs and all four antibody incubation conditions at F620 and F665. Two features of the heat map provide evidence of FRET: (i) the reduction in F620 from cells transfected with both CaSR^{*}875-B1 and CaSR[†]908-B2 and incubated with anti-FLAG:Tb cryptate in either the absence or presence of anti-Myc:XL665; and (ii) the increase in F665 from cells transfected with both CaSR^{*}875-B1 and CaSR[†]908-B2 and incubated with anti-FLAG:Tb cryptate in either the absence or presence of anti-Myc:XL665. Descriptive statistics from 'prior to the full dataset' used to generate the heat map is provided in Table 3. (B) Co-IP experiments: HEK-293 cells were transfected with CaSR^{*}875-B1 alone (lane 1), CaSR[†]908-B2 alone (lane 2), or co-transfected with both CaSR^{*}875-B1 and CaSR[†]908-B2 (lane 3). The protein lysate was immunoprecipitated with anti-FLAG peptide beads. After elution with FLAG peptide, immunoprecipitated proteins were separated by SDS-PAGE followed by electrotransfer to nitrocellulose membranes, which were probed with anti-Myc antibody ($n = 5$). (C) Fluorescence microscopy of cells transfected with FLAG-tagged CaSR875-B1 alone or co-transfected with CaSR908-B2 were labeled for FLAG-tagged receptors and nuclei were stained with DAPI. Scale bars = 10 μ m. TRF = time-resolved fluorescence.

(IP) experiments were performed with CaSR-GABA_B constructs, in which the FLAG (*) or Myc (†) epitopes were inserted between CaSR residues 371 and 372 as above. Lysates from HEK-293 cells co-transfected with CaSR^{*}₈₇₅-B1 and CaSR[†]₉₀₈-B2 were immunoprecipitated using anti-FLAG antibody beads. After elution of immunoprecipitated proteins using soluble FLAG peptide, protein samples were analyzed by SDS-PAGE and Western blotting with anti-cMyc-antibody. In IP (anti-FLAG)-derived protein samples prepared from HEK-293 cells transfected with either CaSR^{*}₈₇₅-B1 or CaSR[†]₉₀₈-B2 alone, no bands were detected using the anti-Myc antibody (Fig. 3B). However, protein samples processed by IP (anti-FLAG) and Western blotting (anti-Myc) and derived from cells co-transfected with both constructs yielded a major band at approximately 300 kDa, corresponding to the expected size of glycosylated CaSR^{*}₈₇₅-B1:CaSR[†]₉₀₈-B2

heterodimers (2072 residues) as well as minor bands at approximately 160 kDa and 140 kDa corresponding to the expected sizes of the two main glycosylated forms of CaSR[†]₉₀₈-B2 monomers (1090 residues).

Taken together the results demonstrate that upon co-expression, CaSR₈₇₅-B1 and CaSR₉₀₈-B2 heterodimers form and are delivered to the cell surface. The results further demonstrate that the trafficking system composed of CaSR₈₇₅-B1 and CaSR₉₀₈-B2 may be used to assess the dimeric requirements for Ca²⁺_o sensing and G protein-mediated signaling, as well as the significance of conformational changes within subunits (*in-cis*) and between subunits (*in-trans*) for signaling.

We proceeded to functional analyses in HEK-293 cells co-transfected with CaSR₈₇₅-B1 and either WTCaSR₉₀₈-B2 or various mutants of CaSR₉₀₈-B2, which, on the background of the

Table 3. Time-Resolved Fluorescence Analysis for Detection of FRET in Receptor Heterodimers

Results	pcDNA3.1	CaSR* ₈₇₅ -B1	CaSR† ₉₀₈ -B2	CaSR* ₈₇₅ -B1& CaSR† ₉₀₈ -B2	Mann-Whitney
F620 nm results					
No antibodies	900 (381, 1567) ¹	758 (283, 1043) ¹	559 (390, 1406) ¹	479 (157, 1012) ¹	
Antibody-1	1797 (1125, 2517) ¹	6123 (2305, 8707) ^{1,3,*}	1241 (909, 2095) ¹	38566 (32902, 41994) ^{1,3,*}	* <i>p</i> < 0.0001
Antibody-2	785 (337, 1051) ²	773 (313, 1261) ²	383 (169, 748) ²	304 (58, 528) ²	
Ab-1 and Ab-2	1513 (1073, 2555) ²	4262 (2307, 6897) ^{2,3}	1300 (793, 1817) ²	32088 (28034, 38461) ^{2,3}	
Kruskal-Wallis	K = 29.3; <i>p</i> < 0.0001	K = 68.4; <i>p</i> < 0.0001	K = 34.9; <i>p</i> < 0.0001	K = 74.2; <i>p</i> < 0.0001	
Mann-Whitney	1. <i>p</i> = 0.0006 2. <i>p</i> = 0.0001	1. <i>p</i> < 0.0001 2. <i>p</i> < 0.0001 3. <i>p</i> = 0.384	1. <i>p</i> = 0.002 2. <i>p</i> < 0.0001	1. <i>p</i> < 0.0001 2. <i>p</i> < 0.0001 3. <i>p</i> = 0.003	
F665 nm results					
No antibodies	371 (213, 759)	369 (129, 690) ¹	200 (114, 700) ¹	189 (95, 457) ¹	
Antibody-1	378 (212, 719)	626 (374, 1042) ^{1,*}	235 (97, 395) ¹	2810 (2281, 3357) ^{1,3,*}	* <i>p</i> < 0.0001
Antibody-2	514 (318, 735)	398 (176, 818) ²	308 (235, 590) ²	457 (284, 772) ²	
Ab-1 and Ab-2	615 (328, 1152)	576 (412, 1262) ²	590 (455, 770) ²	37922 (33481, 41430) ^{2,3}	
Kruskal-Wallis	K = 3.9; <i>p</i> = 0.273	K = 13.7; <i>p</i> = 0.003	K = 17.1; <i>p</i> = 0.0007	K = 82.5; <i>p</i> < 0.0001	
Mann-Whitney		1. <i>p</i> = 0.011 2. <i>p</i> = 0.010	1. <i>p</i> = 0.95 2. <i>p</i> = 0.002	1. <i>p</i> < 0.0001 2. <i>p</i> < 0.0001 3. <i>p</i> < 0.0001	

Fluorescence emission data (counts) at either: (i) 620 nm; or (ii) 665 nm were obtained from HEK-293 cells transfected with DNA constructs as shown. In both cases excitation pulse sequences were performed at 340 nm according to a TRF protocol (see Methods). Although most datasets were normally distributed, several exceptions were noted (Shapiro–Wilk, Kolmogorov–Smirnov, and QQ plot). Accordingly, the data are reported as medians (interquartile ranges), and the non-parametric Kruskal-Wallis test was used to assess differences between the four antibody incubation conditions for each transfectant. Where indicated, the Mann–Whitney post-test was used to compare selected combinations of transfectant: antibody incubation. The data were obtained in 8 experiments performed in triplicate (24 observations). Antibody-1 (Ab-1), anti-FLAG:Tb cryptate; Antibody-2 (Ab-2), anti-Myc:XL665. Superscript numbers (1, 2, or 3) designate comparisons between elements in columns and “*” designates comparisons between elements in rows. “K” is the Kruskal-Wallis statistic.

WTCaSR, disable either Ca²⁺_o sensing and/or cell signaling. Thus we generated selected heterodimers in HEK-293 cells that were composed of CaSR₈₇₅-B1 and CaSR₉₀₈-B2, in which either WT or mutant CaSR sequences were used. They appear below in the following forms (untagged or FLAG-tagged,*): CaSR(WT)₈₇₅-B1 or CaSR*(WT)₈₇₅-B1; CaSR(WT)₉₀₈-B2 or CaSR*(WT)₉₀₈-B2; CaSR(mutant)₈₇₅-B1 or CaSR*(mutant)₈₇₅-B1; and CaSR(mutant)₉₀₈-B2 or CaSR*(mutant)₉₀₈-B2.

Requirements for Ca²⁺_o-dependent VFT domain function by CaSR heterodimers

We first evaluated whether one or both functional CaSR VFT domain(s) were required for Ca²⁺_o-stimulated receptor function, by assessing two well-characterized inactivating mutations, G143E and R185Q.⁽²⁹⁾ In control experiments, the full length CaSR affected by G143E or R185Q exhibited WT levels of total and surface expression but markedly impaired Ca²⁺_o-induced Ca²⁺_i mobilization as described.⁽²⁹⁾ Based on the responses at 30mM Ca²⁺_o, the E_{max} values were ≤10% of WT in both cases (Table 4).

In HEK-293 cells transfected with CaSR*(G143E)₈₇₅-B1 alone or CaSR*(R185Q)₈₇₅-B1 alone, there were no differences in the total expression of either chimera when compared with CaSR*₈₇₅-B1 or CaSR WT, and CaSR*(G143E)₈₇₅-B1 and CaSR*(R185Q)₈₇₅-B1 exhibited similar reductions in surface expression to CaSR*₈₇₅-B1 (Fig. S1). On the other hand, in HEK-293 cells transfected with CaSR*(G143E)₉₀₈-B2 alone or CaSR*(R185Q)₉₀₈-B2 alone, there were no differences in either total or surface expression when compared with CaSR*₉₀₈-B2 (Fig. S2). However, as expected,

receptor function was markedly impaired consistent with the known effects of G143E and R185Q (Table 4).

HEK-293 cells co-transfected with either (i) CaSR(G143E)₈₇₅-B1 and CaSR(G143E)₉₀₈-B2 or (ii) CaSR(R185Q)₈₇₅-B1 and CaSR(R185Q)₉₀₈-B2, respectively, to test for the effects of the *homozygous* mutations G143E/G143E or R185Q/R185Q in the CaSR₈₇₅-B1/CaSR₉₀₈-B2 heterodimer system, exhibited markedly impaired function at Ca²⁺_o up to 30mM, consistent with the expected behavior of dimers in which both subunits contained either G143E or R185Q (Fig. 4A,B; Table 4).

We next examined function in HEK-293 cells co-transfected with either (i) CaSR(WT)₈₇₅-B1 and CaSR(G143E)₉₀₈-B2 or (ii) CaSR(WT)₈₇₅-B1 and CaSR(R185Q)₉₀₈-B2, respectively, to test for the effects of the *heterozygous* mutations WT/G143E or WT/R185Q in the CaSR₈₇₅-B1/CaSR₉₀₈-B2 heterodimer system (Fig. 4A,B; Table 4). Interestingly, robust Ca²⁺_o-stimulated Ca²⁺_i mobilization was observed in HEK-293 cells co-transfected with CaSR(WT)₈₇₅-B1 and either of the two mutant CaSR₉₀₈-B2 constructs, CaSR(G143E)₉₀₈-B2 or CaSR(R185Q)₉₀₈-B2 and the maximal responses were comparable to WTCaSR alone, demonstrating that effective chaperoning of CaSR(WT)₈₇₅-B1 to the cell surface by these functionally-deficient mutant CaSR₉₀₈-B2 receptor proteins was sufficient to restore maximal function (Fig. 4A,B). However, the EC₅₀ values for Ca²⁺_o increased to 11.5 ± 3.3mM for CaSR(WT)₈₇₅-B1/CaSR(G143E)₉₀₈-B2 heterodimers and to 11.6 ± 0.5mM for CaSR(WT)₈₇₅-B1/CaSR(R185Q)₉₀₈-B2 heterodimers when compared with the truncation control CaSR_{876x} (7.5 ± 0.6mM; *n* = 4; Fig. 4). The results demonstrate that within mutant heterodimers, one single functionally-competent VFT domain is sufficient to support maximal levels

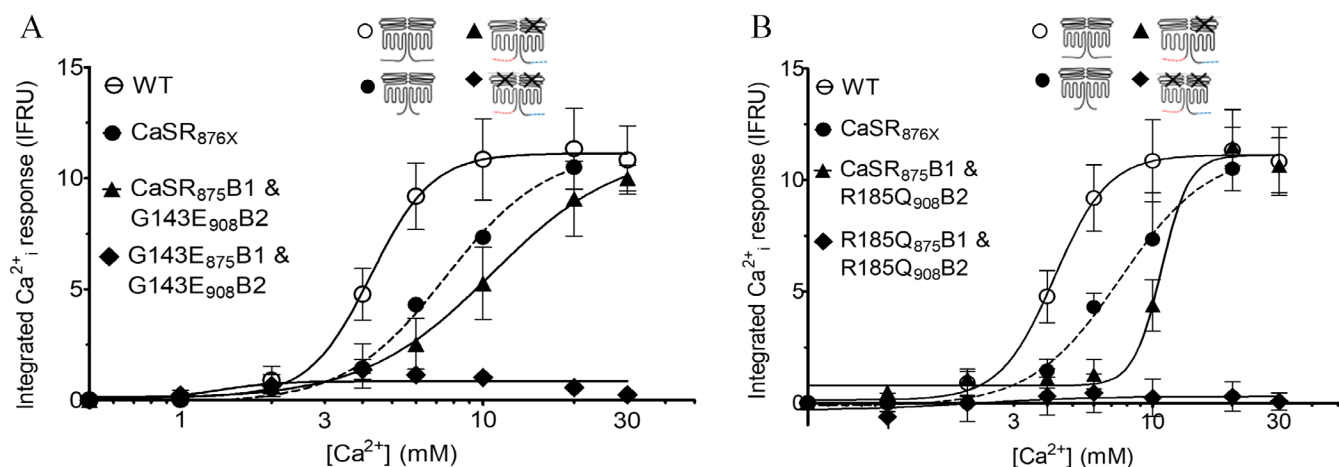


Fig. 4. Functional responses from HEK-293 cells transfected with CaSR-B1 and CaSR-B2 receptor constructs bearing inactivating mutations of the CaSR VFT domain. (A) Ca^{2+}_o -induced Ca^{2+}_i mobilization in Fura2-loaded HEK-293 cells transfected with (i) WTCaSR alone, or (ii) CaSR876X alone, or co-transfected with either (iii) CaSR875-B1 and CaSR(G143E)908-B2, or (iv) CaSR(G143E)875-B1 and CaSR(G143E)908-B2 ($n = 3-6$). (B) Ca^{2+}_o -induced Ca^{2+}_i mobilization in HEK-293 cells transfected with (i) WTCaSR alone, or (ii) CaSR876X alone, or co-transfected with either (iii) CaSR875-B1 and CaSR(R185Q)908-B2, or (iv) CaSR(R185Q)875-B1 and CaSR(R185Q)908-B2 ($n = 3-6$). CaSR(mutant)875-B1 appears as "Mutant875-B1" and CaSR(mutant)908-B2 appears as "Mutant908-B2."

of Ca^{2+}_o -stimulated Ca^{2+}_i mobilization. However, WT levels of Ca^{2+}_o -sensitivity require two functional VFT domains.

HH bundle: G protein interactions

We next used the CaSR₈₇₅-B1/CaSR₉₀₈-B2 trafficking system to investigate the impacts of homozygous and heterozygous mutations of HH bundle associated intraloops that impair coupling to key G proteins, selecting two mutations, F706A in iL-2 and L797A in iL-3, first identified by alanine-scanning mutational analysis,⁽³³⁾

that markedly impair coupling to both $G_{q/11}$ -mediated and $G_{i/o}$ -mediated pathways.^(33,34) Along with the CaSR proximal C-terminus, F706 and L797 support Ca^{2+}_o -stimulated Ca^{2+}_i mobilization.⁽³⁴⁾

Neither F706A nor L797A impaired either total or surface expression of the full-length CaSR in transfected HEK-293 cells as reported.^(33,34) Similarly, neither F706A nor L797A impaired either total or surface expression of CaSR₉₀₈-B2 (Fig. S2). In addition, as expected, both CaSR(F706A)₈₇₅-B1 and CaSR(L797A)₈₇₅-B1 exhibited reduced surface but not total expression, consistent

Table 4. Ca^{2+}_o -Stimulated Responses in Heterodimers Composed of Mutant VFT Domains

Transfection (n)	E_{\max} (IFRU)	pEC_{50} for Ca^{2+}_o (EC_{50} in mM)
WTCaSR (6)	$10.5 \pm 0.7^{1-4}$	$2.45 \pm 0.07 (3.6 \pm 0.5)^{1-4}$
CaSR ₈₇₅ -B1 (4)	0.8 ± 0.9^1	NF
CaSR ₉₀₈ -B2 (6)	$11.9 \pm 1.8^{2,5-8}$	$2.58 \pm 0.13 (2.6 \pm 0.8)^{1,5}$
G143E (3)	1.3 ± 0.2^3	NF
CaSR(G143E) ₉₀₈ -B2 (6)	$2.0 \pm 0.4^{5,9}$	$2.31 \pm 0.15 (4.9 \pm 1.6)^{2,5,6}$
CaSR875-B1 and CaSR(G143E) ₉₀₈ -B2 (6)	$11.5 \pm 3.3^{6,9,10}$	$1.96 \pm 0.17 (11 \pm 4.0)^{3,6}$
CaSR(G143E) ₈₇₅ -B1 and CaSR(G143E) ₉₀₈ -B2 (4)	1.2 ± 0.2^{10}	NF
R185Q (3)	0.6 ± 0.3^4	NF
CaSR(R185Q) ₉₀₈ -B2 (4)	$3.3 \pm 1.5^{7,11}$	NF
CaSR ₈₇₅ -B1 and CaSR(R185Q) ₉₀₈ -B2 (4)	$11.6 \pm 0.5^{8,11,12}$	$1.92 \pm 0.09 (12 \pm 2.5)^4$
CaSR(R185Q) ₈₇₅ -B1 and CaSR(R185Q) ₉₀₈ -B2 (3)	-0.3 ± 0.4^{12}	NF
One-way ANOVA	$F = 19.3; p < 0.0001$	$F = 3.0; p = 0.019$
Welch's post test	1. $p = 0.0002$; 2. $p = 0.68$; 3. $p = 0.0003$; 4. $p = 0.0002$; 5. $p = 0.0011$; 6. $p = 0.52$; 7. $p = 0.0025$; 8. $p = 0.83$; 9. $p = 0.0023$; 10. $p = 0.0020$; 11. $p < 0.0001$; 12. $p < 0.0001$	1. $p = 0.35$; 2. $p = 0.13$; 3. $p = 0.04$; 4. $p = 0.002$; 5. $p = 0.38$; 6. $p = 0.01$

Ca^{2+}_o -induced Ca^{2+}_i mobilization responses were obtained in Fura 2-AM loaded HEK-293 cells that were transfected with the WTCaSR or various mutants. Integrated Ca^{2+}_i responses were fitted to Equation (1) and the data were analyzed in GraphPad Prism. One-way ANOVA demonstrated differences for the maximum values and pEC_{50} values. The data are curve-fit returned values \pm SE. The results of 1-way ANOVA and Welch's t post tests are shown at bottom. Superscript numbers designate comparisons between elements in columns. NF = curve-fit did not permit reliable estimates of pEC_{50} .

with the action of the ER retention motif in the GABA_{B1} C-terminus (Table 5). Co-transfection with CaSR(F706A)₉₀₈-B2 or CaSR(L797A)₉₀₈-B2 was then used to traffic either CaSR₈₇₅-B1 or, respectively, CaSR(F706A)₈₇₅-B1 or CaSR(L797A)₈₇₅-B1 to the cell surface.

Introducing F706A into the WTCaSR reduced the maximal Ca²⁺_i mobilization response by around 40% with no significant change in EC₅₀ for Ca²⁺_o (Fig. 5A; Table 5) as observed.⁽³⁴⁾ The results were similar but more pronounced for L797A, which reduced the maximal response by around 60%–70% (Fig. 5A; Table 5). Similar relative inhibitory effects were observed for F706A and L797A when introduced into CaSR₉₀₈-B2 (Fig. 5B; Table 5).

Cells co-transfected with either (i) CaSR(F706A)₈₇₅-B1 and CaSR(F706A)₉₀₈-B2 (Fig. 5C) or (ii) CaSR(L797A)₈₇₅-B1 and CaSR(L797A)₉₀₈-B2 (Fig. 5D) to deliver *homozygous* mutants to the cell surface exhibited around 60% and 80% suppressions of the E_{max} values, respectively, and similar approximately 60% and 80% suppressions, respectively, were obtained in cells co-transfected with either (i) CaSR(WT)₈₇₅-B1 and CaSR(F706A)₉₀₈-B2 (Fig. 5C) or (ii) CaSR(WT)₈₇₅-B1 and CaSR(L797A)₉₀₈-B2 (Fig. 5D) to deliver *heterozygous* mutants to the cell surface. Thus,

the heterozygous mutants exhibited comparable suppressions of the maximal responses, demonstrating that the loss of one of the two available functional G protein coupling domains is sufficient to induce maximal disruption of CaSR signaling. Thus, there were no significant differences in E_{max} or EC₅₀ for Ca²⁺_o according to whether either F706A or L797A was present in just one or both heterodimeric subunits (Table 5).

These results demonstrate that a minimum of two functional HH bundles and associated intraloop networks are required for efficient G protein coupling in Ca²⁺_o-stimulated Ca²⁺_i mobilization. Furthermore, the presence of one WT HH bundle was insufficient to provide even partial compensation for the loss of the intraloop network in its neighboring subunit.

Cis/trans signal transmission from the VFT domains to HH bundles

We next investigated how Ca²⁺_o-dependent activation of the VFT domains couples to G protein-dependent signaling via the intraloops in CaSR dimers. To assess this, we used the mutation G143E in the VFT domain and L797A in iL-3 to deliver mutant

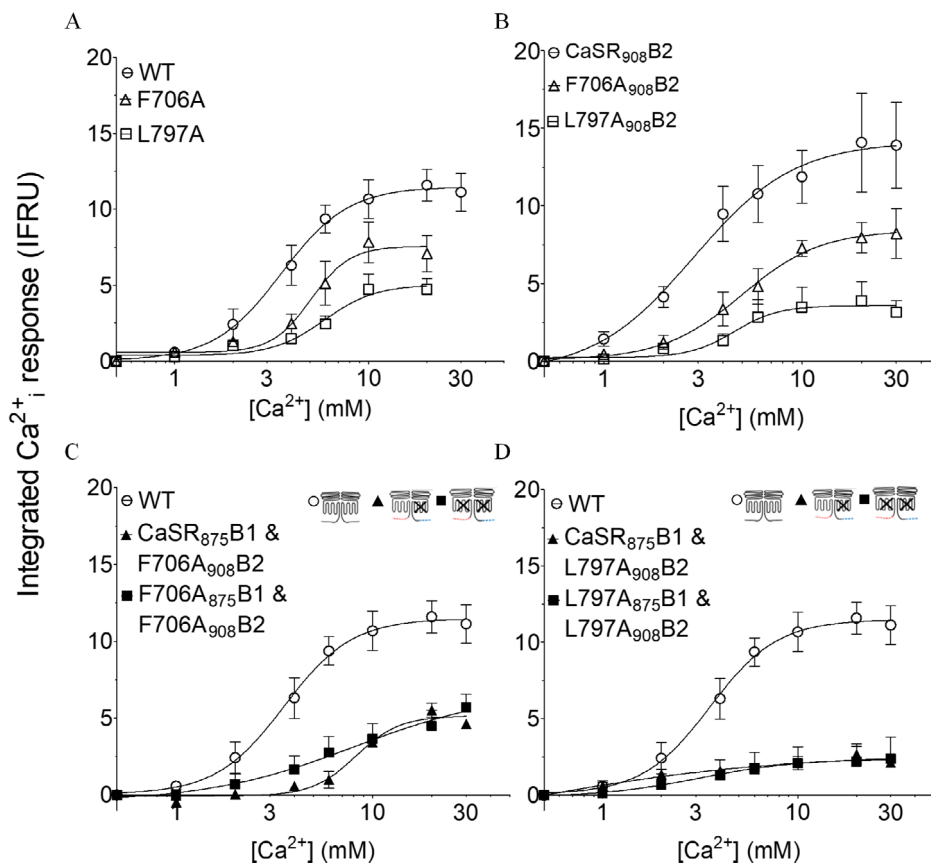


Fig. 5. Functional responses in HEK-293 cells transfected with CaSR-B1 and CaSR-B2 chimeras bearing inactivating mutations of CaSR iL-2 or iL-3. (A) Ca²⁺_o-induced Ca²⁺_i mobilization in Fura2-loaded HEK-293 cells transfected with (i) WTCaSR, (ii) CaSR(F706A), or (iii) CaSR(L797A). (B) Ca²⁺_o-induced Ca²⁺_i mobilization in Fura2-loaded HEK-293 cells transfected with (i) CaSR₉₀₈-B2, (ii) CaSR(F706A)₉₀₈-B2, or (iii) CaSR(L797A)₉₀₈-B2. (C) Ca²⁺_o-induced Ca²⁺_i mobilization in Fura2-loaded HEK-293 cells co-transfected with either (i) CaSR₈₇₅-B1 and CaSR(F706A)₉₀₈-B2 or (ii) CaSR(F706A)₈₇₅-B1 and CaSR(F706A)₉₀₈-B2. (D) Ca²⁺_o-induced Ca²⁺_i mobilization in Fura2-loaded HEK-293 cells co-transfected with either (i) CaSR₈₇₅-B1 and CaSR(L797A)₉₀₈-B2 or (ii) CaSR(L797A)₈₇₅-B1 and CaSR(L797A)₉₀₈-B2 (n = 3–5). CaSR(mutant)₈₇₅-B1 appears as “Mutant875-B1” and CaSR(mutant)₉₀₈-B2 appears as “Mutant908-B2.”

Table 5. Ca²⁺_o-Stimulated Responses in Heterodimers Composed of Mutant HH Bundles

Transfection (n)	E _{max} (IFRU)	pEC ₅₀ for Ca ²⁺ _o (EC ₅₀ in mM)
WTCaSR (8)	11.5 ± 0.7 ¹⁻³	2.45 ± 0.06 (3.6 ± 0.5) ¹⁻³
CaSR ₉₀₈ -B2 (6)	12.0 ± 1.5 ^{1,4,5}	2.58 ± 0.12 (2.7 ± 0.7) ^{1,4,5}
F706A (7)	6.9 ± 1.0 ²	2.32 ± 0.07 (4.8 ± 0.8) ²
CaSR(F706A) ₉₀₈ -B2 (3)	8.4 ± 0.8 ⁴	2.30 ± 0.08 (5.0 ± 0.9) ⁴
CaSR ₈₇₅ -B1 and CaSR(F706A) ₉₀₈ -B2 (4)	4.6 ± 0.5 ⁶	2.10 ± 0.06 (8.0 ± 1.2) ⁶
CaSR(F706A) ₈₇₅ -B1 and CaSR(F706A) ₉₀₈ -B2 (3)	5.1 ± 1.3 ⁶	2.26 ± 0.17 (5.6 ± 2.1) ⁶
L797A (8)	5.1 ± 0.9 ³	2.21 ± 0.09 (6.0 ± 1.3) ³
CaSR(L797A) ₉₀₈ -B2 (3)	3.6 ± 0.5 ⁵	2.33 ± 0.10 (4.6 ± 1.1) ⁵
CaSR ₈₇₅ -B1 and CaSR(L797A) ₉₀₈ -B2 (4)	2.3 ± 0.2 ^{*7}	2.73 ± 0.13 (1.9 ± 0.6) [*]
CaSR(L797A) ₈₇₅ -B1 and CaSR(L797A) ₉₀₈ -B2 (3)	2.4 ± 0.9 ⁷	2.50 ± 0.43 (3.2 ± 3.1)
One-way ANOVA	F = 6.3; p < 0.0001	F = 3.0; p = 0.02
Welch's t post tests	1. p = 0.97; 2. p = 0.04; 3. p = 0.0005; 4. p = 0.24; 5. p = 0.008; 6. p = 0.46; 7. p = 0.88	1. p = 0.20; 2. p = 0.16; 3. p = 0.09; 4. p = 0.19; 5. p = 0.04; 6. p = 0.32

Ca²⁺_o-induced Ca²⁺_i mobilization responses were obtained in Fura 2-AM loaded HEK-293 cells that were transfected with the WTCaSR or various mutants. Integrated Ca²⁺_i responses were fitted to Equation (1) and the data were analyzed in GraphPad Prism. One-way ANOVA demonstrated differences for the maximum values and pEC₅₀ values. The data are curve-fit returned values ± SE. The results of one-way ANOVA and Welch's t post test are shown at in the bottom row. Superscript numbers designate comparisons between elements in columns.

*Hill coefficient fixed to wild-type value to permit curve-fit.

heterodimers to the cell surface based on the CaSR₈₇₅-B1/CaSR₉₀₈-B2 trafficking system. Three distinct possibilities for the mechanism of signal transmission seem feasible within receptor dimers, via: (i) the HH bundle within the same subunit (*in-cis*); (ii) the HH bundle of the neighboring subunit (*in-trans*); or (iii) a combination of both these mechanisms. Previous studies have demonstrated that signaling in CaSR dimers is supported, at least in part, via robust *trans*-based interactions between the VFT domain of one subunit and HH bundle of its neighboring subunit but have not excluded the co-existence of *cis*-dependent contributions.^(11,17)

We first investigated the ability of the VFT domain to activate its own HH bundle by introducing the double mutation G143E/

L797A into CaSR₉₀₈-B2 to impair the functions of both VFT domain (Ca²⁺-sensing; G143E) and iL-3 (G protein-coupling; L797A) within the same subunit. HEK-293 cells transfected alone with CaSR(G143E/L797A)₉₀₈-B2 homodimers had markedly impaired signaling with E_{max} for Ca²⁺_o-induced Ca²⁺_i mobilization suppressed to around 10%–20% of the WTCaSR (Fig. 6A; Table 6). Interestingly, HEK-293 cells co-transfected with CaSR(G143E/L797A)₉₀₈-B2 and CaSR(WT)₈₇₅-B1 exhibited markedly impaired Ca²⁺_o-induced Ca²⁺_i mobilization that was indistinguishable from cells singly transfected with CaSR(G143E/L797A)₉₀₈-B2 (Fig. 6A; Table 6). Taken together the results demonstrate that signal transmission within Ca²⁺_o-stimulated CaSR dimers is not supported by VFT domain-HH bundle-based

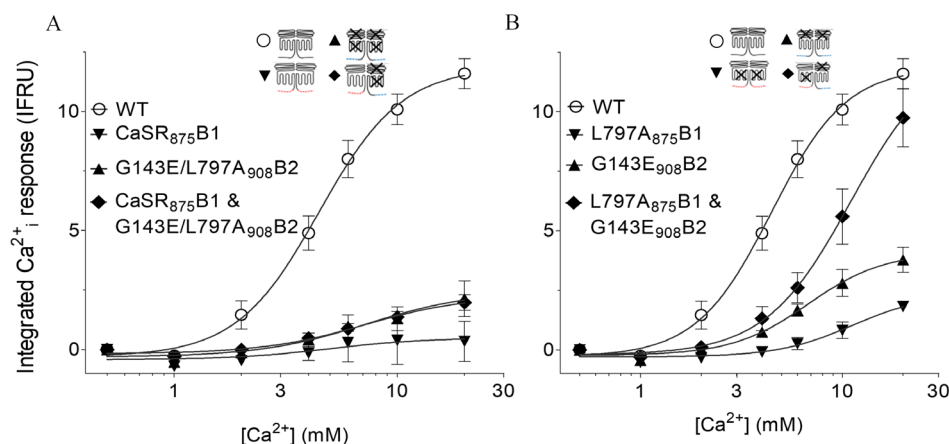


Fig. 6. Evidence for signaling *in-trans* but not *in-cis* within CaSR heterodimers. Ca²⁺_o-stimulated Ca²⁺_i mobilization in Fura2-loaded HEK-293 cells transfected with various CaSR mutants. Concentration-response curves were obtained by integration of raw data and curve fitting to Equation (1). (A) Single transfections of (i) CaSR₈₇₅-B1, (ii) CaSR(G143E/L797A)₉₀₈-B2, or (iii) both, to test for signaling *in-cis* (sensing and signaling via CaSR₈₇₅-B1). (B) Single transfections of (i) CaSR(L797A)₈₇₅-B1, (ii) CaSR(G143E)₉₀₈-B2, or (iii) both to test for signaling *in-trans* (sensing via CaSR(L797A)₈₇₅-B1 and signaling via CaSR(G143E)₉₀₈-B2). Only signaling *in-trans* was observed (n = 3). CaSR(mutant)₈₇₅-B1 appears as “Mutant875-B1” and CaSR(mutant)₉₀₈-B2 appears as “Mutant908-B2.”

Table 6. Analysis for Signaling *in-cis* or *in-trans* Between VFT and HH Bundles

Transfection (n)	E _{max} (IFRUs)	pEC ₅₀ for Ca ²⁺ _o (EC ₅₀ in mM)
WTCaSR (8)	11.9 ± 0.8 ¹⁻⁶	2.35 ± 0.04 ¹⁻⁶ (4.5 ± 0.4)
CaSR ₈₇₅ -B1 (2)	0.4 ± 0.5 ¹	2.36 ± 0.31 ¹ (4.4 ± 3.1)
CaSR (G143E/L797A) ₉₀₈ -B2 (5)	2.5 ± 1.3 ²	2.14 ± 0.27 ² (7.3 ± 4.4)
CaSR ₈₇₅ -B1 and CaSR (G143E/L797A) ₉₀₈ -B2 (8)	2.3 ± 0.6 ³	2.15 ± 0.14 ³ (7.1 ± 2.3)
CaSR (L797A) ₈₇₅ -B1 (5)	2.3 ± 1.0 ⁴	1.95 ± 0.18 ⁴ (11.2 ± 4.6)
CaSR (G143E) ₉₀₈ -B2 (9)	4.1 ± 0.6 ⁵	2.17 ± 0.08 ⁵ (6.8 ± 1.3)
CaSR (L797A) ₈₇₅ -B1 and CaSR (G143E) ₉₀₈ -B2 (8)	12.6 ± 4.0 ⁶	1.96 ± 0.16 ⁶ (11.0 ± 4.1)
One-way ANOVA	F = 30.1; p < 0.0001	F = 8.16; p < 0.0001
Welch's t post test	1. p = 0.01; 2. p = 0.0005; 3. p < 0.0001 4. p < 0.0001; 5. p = 0.0001; 6. p = 0.73	1. p = 0.50; 2. p = 0.22; 3. p < 0.0001 4. p = 0.02; 5. p = 0.10; 6. p = 0.0005

Ca²⁺_o-induced Ca²⁺_i mobilization responses were obtained in Fura 2-AM loaded HEK-293 cells that were transfected with the WTCaSR or various mutants. CaSR(G143E/L797A)₉₀₈-B2, affected by mutations of both the VFT and the HH bundle, was used to test for signaling *in-cis* when co-expressed with CaSR₈₇₅-B1. CaSR(L797A)₈₇₅-B1 and CaSR(G143E)₉₀₈-B2 were co-expressed to test for signaling *in-trans*. Integrated Ca²⁺_i responses were fitted to Equation (1) and the data were analyzed in GraphPad Prism. One-way ANOVA demonstrated differences between groups for E_{max} and pEC₅₀. The data are curve-fit returned values ± SE. The results of one-way ANOVA and Welch's t posttests are shown at bottom. Superscript numbers designate comparisons between elements in columns.

interactions within subunits (ie, *in-cis*) and is thus entirely dependent on interactions between subunits across the dimer interface (ie, *in-trans*).

To confirm the critical importance of *in-trans* signaling we investigated Ca²⁺_o-stimulated Ca²⁺_i mobilization in HEK-293 cells transfected with either CaSR(L797A)₈₇₅-B1 or CaSR(G143E)₉₀₈-B2 alone or co-transfected with both chimeras. In these experiments, signaling *in-cis* was unavailable in homodimers in the cases of either B1:B1 (expression and signaling impaired) or B2:B2 (Ca²⁺_o sensing impaired), but signaling *in-trans* was available in B1:B2 heterodimers whereby CaSR(L797A)₈₇₅-B1 provided an intact VFT domain and CaSR(G143E)₉₀₈-B2 provided an intact HH bundle signaling unit. As expected, HEK-293 cells transfected alone with either CaSR(L797A)₈₇₅-B1 or CaSR(G143E)₉₀₈-B2 exhibited markedly impaired Ca²⁺_o-induced Ca²⁺_i mobilization (E_{max} values ~20% and 35% of WTCaSR; Fig. 6B; Table 6). Interestingly, however, cells co-transfected with CaSR(L797A)₈₇₅-B1 and CaSR(G143E)₉₀₈-B2 exhibited E_{max} values comparable to those observed in cells transfected with the WTCaSR, demonstrating signal transmission *in-trans* between the intact VFT domain in CaSR(L797A)₈₇₅-B1 and intact HH bundle in CaSR(G143E)₉₀₈-B2, consistent with previous reports.^(11,17)

These findings demonstrate that in the Ca²⁺_o-stimulated WTCaSR, functionally important molecular interactions within dimers occur *in-trans*; ie, between subunits. Nevertheless, signal transmission from the CaSR VFT to HH bundle via a single *trans* pathway in cells co-transfected with CaSR(L797A)₈₇₅-B1 and CaSR(G143E)₉₀₈-B2 was not sufficient to support WT levels of Ca²⁺_o sensitivity (Table 3), arising presumably from the loss of the second *in-trans* signaling pathway between the VFT domain of CaSR(G143E)₉₀₈-B2 and HH bundle of CaSR(L797A)₈₇₅-B1.

Effect of G_{q/11} inhibitor on Ca²⁺_o-stimulated IP₁ responses in WT CaSR and mutant heterodimers

We further investigated the signaling responses from the WT CaSR and two mutant heterodimers, (i) CaSR₈₇₅-B1:CaSR (G143E)₉₀₈-B2 (representing heterodimers with an impaired VFT sensing domain) and (ii) CaSR₈₇₅-B1:CaSR(L797A)₉₀₈-B2 (representing heterodimers with an impaired signaling domain) in the absence or presence of the cell-permeant, selective G_{q/11} inhibitor, YM-254890, and using IP₁ generation as the readout. The WT CaSR induced a robust Ca²⁺_o concentration-dependent

response with an EC₅₀ value of 3.0 ± 0.8mM (n = 4). The response was almost abolished by incubation in the presence of YM-254890 (0.5μM; Fig. S3A). As in the case of Ca²⁺_i mobilization, we observed partial recovery of function in Ca²⁺_o-stimulated IP₁ generation in cells transfected to generate CaSR₈₇₅-B1:CaSR(G143E)₉₀₈-B2 heterodimers, which, like WT, was markedly inhibited by YM-254890 (Fig. S3B). However, cells transfected with CaSR₈₇₅-B1:CaSR(L797A)₉₀₈-B2 exhibited no IP₁ response (Fig. S3C), demonstrating that G_{q/11} function is eliminated even in the heterozygous state, consistent with the findings that there was no gene dosage effect for this class of mutants.

Discussion

In this study we investigated the impacts of heterozygous as well as homozygous inactivating mutations of (i) VFT Ca²⁺_o sensing domains and (ii) HH bundle iL signaling domains on dimeric CaSR function, concluding that gene dosage effects impact VFT domain-dependent Ca²⁺_o sensing but not iL-dependent signaling. Thus heterozygous mutations were clearly less severe than homozygous mutations of the VFT domains but of comparable severity in the cases of the iL signaling domains. We also set out to investigate whether Ca²⁺_o-stimulated signaling in receptor dimers might utilize an *in-cis* mechanism as well as the *in-trans* mechanism as reported,^(11,17) concluding that Ca²⁺_o-stimulated signaling operates exclusively via an *in-trans* mechanism.

To permit us to address these questions, we successfully developed a system for delivering CaSR heterodimers to the cell surface using the GABA_B sorting system in a manner similar to that described.⁽³¹⁾ This represents an advance on approaches used hitherto in studies of the CaSR based on co-expression of: (i) WT and mutant receptors, in which the analysis was confounded by the co-existence of a pool of WT homodimers^(28,29); or (ii) mutants affecting the Ca²⁺_o sensing or signaling domains that limited analyses of gene dosage effects and of a possible complementary role for signaling *in-cis* along with signaling *in-trans*.^(11,17) The two key components of the system we developed were as follows: (i) a CaSR subunit truncated after residue S875, to which was appended the C-terminus of GABA_{B1}; and

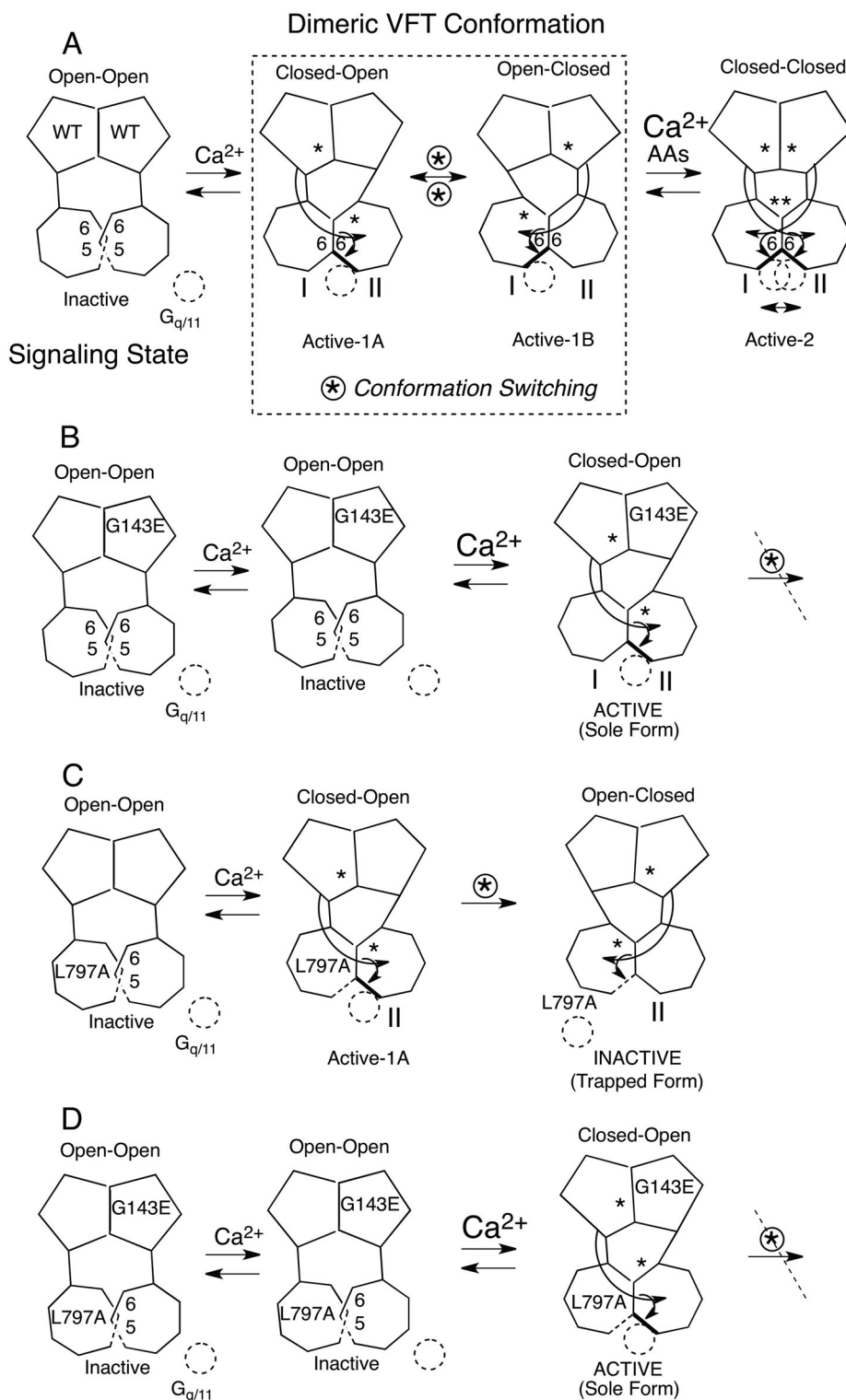


Fig. 7. Model for the impacts of heterozygous mutants, and basis of *in-trans* signaling. The CaSR with dimeric VFT domain units (pentagons at top) interacts via CR domains (solid lines) with HH bundles (heptagons at bottom). Ca²⁺ is an agonist. L-AAs are positive modulators. Two VFT subunit conformations are recognized, “Open” (regular pentagons) and “Closed” (pentagons distorted to extend the dimer interface and appose neighboring HH bundles). Dimeric VFT units may be either (i) Inactive (Open-Open), or (ii) Active (Closed-Open, Open-Closed, or Closed-Closed). Two distinct G protein binding sites (I and II) are shown, one per subunit. Active sites are shown in bold. Mutant sites (deactivated) are represented by dotted lines. The molecular bases for function are considered for Ca²⁺-stimulated (Fig. 7A) WT homodimers and then (Fig. 7B) heterozygous G143E, (Fig. 7C) heterozygous L797A, and (Fig. 7D) CaSR(L797A)875-B1: CaSR(G143E)908-B2 heterodimers operating in *trans*. *Denotes activation. In the Inactive state, dimeric HH bundles are organized so that TMDs 5 and 6 in Subunit-I, and TMDs 5' and 6' in Subunit-II form the interface. In Active states, rotational rearrangements in neighboring HH bundles closely appose TMD-6 and TMD-6'. We propose that *in-trans* (Figure legend continues on next page.)

(ii) a CaSR subunit truncated after residue S908, to which was appended the C-terminus of GABA_{B2}. Appending the GABA_{B1} C-terminal peptide impaired surface expression of all CaSR constructs tested (Table 1) associated with enhanced perinuclear localization on confocal microscopy (Fig. 1B). These findings are consistent with retention of CaSR-GABA_{B1} chimeras in the ER.

The choice of the truncation after S875 in the preferred CaSR-B1 construct (ie, CaSR₈₇₅-B1) appears to have been critical. Despite WT-like levels of total and surface expression, HEK-293 cells transfected with CaSR_{866X} were nonfunctional (Fig. 1, Table 1), consistent with previous studies showing that proximal C-terminal residues between 863 and 874 are required not for expression, but for receptor-induced PI-PLC activation and Ca²⁺_i mobilization,^(34,42,44) and resistance to desensitization.⁽⁴³⁾ HEK-293 cells transfected with CaSR_{876X}, however, exhibited WT-like levels of total and surface expression together with Ca²⁺_o-induced Ca²⁺_i mobilization with a maximum response that was comparable to WT. HEK-293 cells transfected with CaSR₈₇₅-B1, on the other hand, exhibited complete loss of Ca²⁺_o-induced Ca²⁺_i mobilization together with a marked impairment of cell surface expression dependent on the recognized ER retention motif *RSRR* (GABA_{B1} residues 922–925; Fig. 3, Table 2).

Upon co-transfection with CaSR₉₀₈-B2, surface expression of CaSR₈₇₅-B1 was restored to a level comparable to that observed in cells transfected with either the WTCaSR or CaSR_{876X} (Table 1 and 3), and was dependent on the formation of CaSR₈₇₅-B1:CaSR₉₀₈-B2 heterodimers as revealed by TRF and Co-IP analysis (Fig. 3, Table 3). In the case of the TRF experiments it was necessary to wash the cells expressing CaSR subunits by centrifugation to reduce background fluorescence from labeled antibodies in the bulk medium as well as nonspecific binding at the cell surface. Under these circumstances, we observed the expected reduction in donor emission from Tb-cryptate labeled anti-FLAG antibody in cells co-transfected with CaSR^{*}₈₇₅-B1 and CaSR⁺₉₀₈-B2 upon co-incubation with the FRET acceptor XL665-labeled anti-c-Myc antibody (Fig. 3A, Table 3). In addition, the function of CaSR₈₇₅-B1:CaSR₉₀₈-B2 heterodimers was comparable to that observed in cells transfected with CaSR_{876X}. Finally, despite apparent impairments in surface expression in both cases, HEK-293 cells transfected with CaSR₈₉₀-B1 or CaSR₉₀₈-B1 exhibited only approximately 40% reductions in their maximum responses indicating that the ER retention signal in the GABA_{B1} C-terminus was at least partially overcome by CaSR residues 876–890 in both constructs. The overlapping CaSR C-terminal peptide 874–888 has been reported to promote cell surface expression,⁽⁴²⁾ and may arise from a limited region of alpha-helix (residues 877–891).⁽⁴⁴⁾ It is possible that forward trafficking positioned the

receptor in a submembrane vesicle population that was not detected by the surface expression assay but was capable of supporting Ca²⁺_i mobilization. Consistent with this notion, cells transfected with CaSR₈₉₀-B1 or CaSR₉₀₈-B1 exhibited CaSR staining patterns suggesting both perinuclear/ER and sub-plasma membrane localization, whereas cells transfected with CaSR₈₇₅-B1 or CaSR₈₆₅-B1 exhibited staining that was predominantly perinuclear/ER (Fig. 1B). Thus, when co-expressed with CaSR₉₀₈-B2, of the four CaSR C-termini (–865, –875, –890, and –908) tested in CaSR-B1 constructs, only CaSR₈₇₅-B1 was suitable for the selective delivery of functionally competent CaSR heterodimers to the cell surface (Figs. 1 and 3; Table 2).

Although we succeeded in delivering CaSR₈₇₅-B1:CaSR₉₀₈-B2 heterodimers and not CaSR₈₇₅-B1:CaSR₈₇₅-B1 homodimers to the cell surface, the sorting system could not prevent the formation and delivery of CaSR₉₀₈-B2:CaSR₉₀₈-B2 homodimers, which were readily trafficked to the cell surface (Table 1). Based on equal total protein levels for CaSR₈₇₅-B1 and CaSR₉₀₈-B2 subunits, the expected stoichiometry at the cell surface of CaSR₈₇₅-B1:CaSR₉₀₈-B2 heterodimers relative to CaSR₉₀₈-B2:CaSR₉₀₈-B2 homodimers is 2:1. In this respect the system resembled that described by Kniazeff and colleagues,⁽³¹⁾ but not Brock and colleagues,⁽⁴⁵⁾ who succeeded in suppressing the trafficking of modified mGlu₅-B2 subunits to the cell surface, which were released in the presence of modified mGlu₅-B1 subunits. In pilot experiments we attempted unsuccessfully to refine the CaSR₈₇₅-B1:CaSR₉₀₈-B2 system in a similar manner. Thus, we were limited in the way in which we could use the receptor trafficking system. In particular, it was necessary to introduce mutations into CaSR₉₀₈-B2 that markedly impaired the function of homodimers but might be rescued functionally in heterodimers with CaSR₈₇₅-B1. Nevertheless, we were able to assess the relative importance of heterozygous versus homozygous mutations of the dimeric VFT domains and HH bundle intraloops, and to assess the potential role of signaling *in-cis* in combination with the established *in-trans* mechanism^(11,17).

Signaling analyses

We focused on Ca²⁺_o-induced Ca²⁺_i mobilization in the present studies as a well-recognized readout for the CaSR⁽⁴⁶⁾ that is dependent on the key G_{q/11} proteins.^(47,48) However, to investigate whether the observed behavior was representative of CaSR-mediated activation of PI-PLC we also investigated the impacts of the WT CaSR and two heterozygous mutant heterodimers, (i) CaSR(WT)₈₇₅-B1:CaSR(G143E)₉₀₈-B2 and (ii) CaSR(WT)₈₇₅-B1:CaSR(L797A)₉₀₈-B2 on IP₁ generation in the absence or presence of the selective G_{q/11} inhibitor YM-254890. The results

(Figure legend continued from previous page.)

coupling arises via asymmetric arrangements (long curved arrows), whereby activation of G protein Site-II (Subunit II) occurs in response to VFT domain closure in Subunit-I and in the following cycle, activation of G protein Site-I occurs in response to closure of the VFT domain of Subunit-II. Note in A the transition from Active-1A to Active-1B requires a Conformational Switch (eg, by phosphorylation of S875 and/or T888) that might work by driving alternating asymmetry at the HH bundle dimer interface, as reported.⁽¹⁴⁾ In B, heterozygous mutation G143E resists adoption of the Closed-Open (1A) or Open-Closed (1B) active states. At higher Ca²⁺ concentrations, however, the dimeric VFT unit adopts the Closed-Open (Active-1A) form, which is stably active, but G143E in Subunit-II impedes transition to the Open-Closed form. In C, heterozygous mutation L797A does not prevent the formation of the Closed-Open form in response to Ca²⁺ or attendant G protein coupling to Subunit-II and receptor function (Active-1A). Conformational switching then drives the formation of an Open-Closed form that is stably inactive because failure of signaling prevents further conformational switching. In D, heterodimers formed by CaSR(G143E)₉₀₈-B2:CaSR(L797A)₈₇₅-B1 are inactive at lower Ca²⁺ concentrations as in B and retain signaling at higher Ca²⁺ by adopting a stable Closed-Open conformation. Although conformational switching is elaborated by subunit-II, it fails to switch the receptor to the Open-Closed state due to G143E. AA = amino acid.⁽⁶²⁾

identify $G_{q/11}$ as a key G protein downstream of the WT CaSR in HEK-293 cells and for CaSR(WT)₈₇₅-B1:CaSR(G143E)₉₀₈-B2 heterodimers. Interestingly, however, CaSR(WT)₈₇₅-B1:CaSR(L797A)₉₀₈-B2 heterodimers were inactive in the assay up to a Ca^{2+}_o concentration of 20mM, demonstrating that the iL-3 mutant disables $G_{q/11}$ -dependent signaling even in the heterozygous state; ie, lack of gene dosage.

In various tissue and cell types, the CaSR couples to G proteins other than $G_{q/11}$ and also to β -arrestin (reviewed in Ref. 10). Whether heterozygous dimers with iL-3 mutations impair coupling to alternative signaling pathways requires further study.

VFT domain mutants exhibit gene dosage effects

To assess the requirements for Ca^{2+}_o sensing we selected G143E and R185Q, two naturally occurring inactivating VFT domain mutations, which markedly impair function in mutant homodimers.^(17,29) Cells that expressed only homodimers composed of CaSR(G143E)₉₀₈-B2 or CaSR(R185Q)₉₀₈-B2 exhibited markedly suppressed Ca^{2+}_o -induced responses (Table 4). On the other hand, cells that also expressed WT-mutant heterodimers formed of (i) CaSR(WT)₈₇₅-B1 and CaSR(G143E)₉₀₈-B2 or (ii) CaSR(WT)₈₇₅-B1 and CaSR(R185Q)₉₀₈-B2 exhibited robust Ca^{2+}_i mobilization with maximum responses that were not significantly different from WT and EC_{50} values for Ca^{2+}_o , which were only mildly-moderately increased when compared to the control construct, CaSR_{876X} (Fig. 4). The increases observed in the EC_{50} values for Ca^{2+}_o are consistent with the identified roles of G143E and R185Q in the etiology of familial hypocalciuric hypercalcemia type-1 (FHH-1) in some human kindreds.^(29,49) Unlike mutant heterodimers that were *heterozygous* for G143E or R185Q, which retained significant CaSR activity, mutant heterodimers that were *homozygous* for G143E or R185Q were non-functional (Fig. 4). The results demonstrate the existence of a pronounced gene dosage effect for VFT domain mutants. In the context of FHH-1, this gene dosage effect might arise from heterodimers, in which a subunit with a WT VFT domain partially compensates for a partner subunit disabled by a VFT domain mutation, as well as a residual pool of fully functional WT homodimers.

In relating these findings to the recently solved inactive and active structures of the CaSR extracellular domain and the inferred mechanism of receptor activation it is necessary to consider the key events that underlie receptor activation including: (i) closure of the VFT domain; (ii) stabilization of the closed VFT domain; and (iii) the consequent apposition of neighboring HH bundles.⁽²³⁾ For a mutation that impairs closure of a single VFT domain it seems likely that the formation of Ca^{2+}_o sites that stabilize the closed/active state will also be impaired, thereby reducing Ca^{2+}_o potency/sensitivity. If full closure of the mutant VFT domain can occur, albeit at higher Ca^{2+}_o , the observed WT maximum response together with impaired Ca^{2+}_o potency can be explained.

As noted above, the choice of CaSR₈₇₅-B1 in partnership with CaSR₉₀₈-B2 was critical for the delivery of mutant heterodimers to the cell surface that were functionally active in Ca^{2+}_o -stimulated Ca^{2+}_i mobilization assays. It is pertinent to note that although the two key PKC-dependent phosphorylation sites at T888⁽⁵⁰⁾ and S875⁽⁵¹⁾ were both intact in one of these constructs, CaSR₉₀₈-B2, it seems likely that neither of the phosphorylation sites was active in CaSR₈₇₅-B1, in which T888 was deleted and in which S875, although present, may not have been recognized by PKC due to the loss of the immediate C-terminal peptide,

residues 876–879 TAAH. A loss of all four PKC sites in receptor homodimers promotes receptor activity via enhanced Ca^{2+}_o sensitivity⁽⁵¹⁾ and T888M is a known activating mutation in humans.⁽⁵²⁾ However, it is possible that the presence of two intact sites on one subunit (ie, CaSR₉₀₈-B2) is sufficient to negatively modulate the Ca^{2+}_o sensitivity of receptor dimers.

HH bundle intraloop inactivating mutants do not exhibit gene dosage effects

To assess the requirements for HH bundle-mediated signaling we selected two inactivating mutations of the CaSR intraloops, F706A in iL-2 and L797A in iL-3. Both these mutations impair Ca^{2+}_o -stimulated signaling via PI-PLC and Ca^{2+}_i mobilization^(33,34) and lie close to previously identified human FHH-1 mutations in iL-2, R701P⁽⁵³⁾ and in iL-3, R795W,⁽²⁹⁾ and P798T/L,⁽⁵³⁾ respectively. Regardless of whether the background was the WTCaSR or CaSR₉₀₈-B2 both F706A and L797A markedly impaired maximal Ca^{2+}_o -stimulated Ca^{2+}_i mobilization by around 40% and 60%, respectively (Fig. 5). Interestingly, similar effects were observed when CaSR(F706A)₉₀₈-B2 or CaSR(L797A)₉₀₈-B2 were co-expressed with CaSR₈₇₅-B1, demonstrating that in the heterodimers, the WT intraloops in CaSR₈₇₅-B1 were unable to compensate for the inactivating intraloop mutants. Furthermore, co-expression of CaSR(F706A)₈₇₅-B1 or CaSR(L797A)₈₇₅-B1 with CaSR(F706A)₉₀₈-B2 or CaSR(L797A)₉₀₈-B2, respectively, had no further inhibitory effect (Fig. 5). Thus the loss of one functional intraloop maximally disables signaling.

Recent work has suggested that class C GPCRs support one heterotrimeric G protein molecule per receptor dimer.⁽¹¹⁻¹³⁾ From this perspective, both sets of intraloops appear to be required for sequential docking and activation of G proteins by receptor dimers, and it seems plausible that together two HH bundles create just one G protein binding site. Finally, it should be noted that a gene dosage effect was reported for the *activating* iL-2 mutation L723Q in the *Nuf* mouse.⁽⁵⁴⁾ The present results suggest that inactivating and activating mutations of the CaSR intraloops are distinct not only with respect to their impact on signaling; ie, decreased or increased, but also with respect to the underlying mechanism.

Dominant-negative behavior in mutant CaSR heterodimers

Previously, two CaSR mutants, R185Q and R795W were identified as “dominant negatives,” acting to suppress endogenous CaSR signaling in cultured cells.^(29,55) The results of the present study indicate that the mechanisms of action of these two mutants are distinct. In the case of R185Q (gene dosage), overexpression of the mutant in cells that express WT CaSR has the effect of shifting the Ca^{2+}_o concentration response curves to the right as the proportion of CaSR homodimers falls and the proportions of WTCaSR: CaSR(R185Q) heterodimers and CaSR(R185Q) mutant homodimers rise. Because mutant homodimers are non-functional in the case of R185Q (Fig. 4B), cellular receptor function in heterozygotes should depend on the absolute and relative levels of WTCaSR: CaSR(R185Q) heterodimers and WT homodimers. Overexpression of R795W, on the other hand, which lies close to L797 in iL-3, is expected to suppress the receptors' maximum responses as the proportion of WT homodimers falls and the proportion of disabled and functionally-comparable WTCaSR: CaSR(R795W) heterodimers and CaSR(R795W) mutant homodimers rises.

Only trans-dependent activation supports Ca^{2+}_o -stimulated Ca^{2+}_i mobilization

Our studies support and extend previous conclusions that the Ca^{2+}_o -stimulated CaSR requires signaling *in-trans* between the VFT domain of one subunit and the HH bundle of its partner subunit.^(11,17) Thus, when expressed singly, neither CaSR(G143E)₉₀₈-B2 nor CaSR(L797A)₈₇₅-B1 was able to support WT maximum levels of Ca^{2+}_o -stimulated Ca^{2+}_i responses (Fig. 6B). However, when these two mutant chimeras were co-expressed under conditions in which heterodimers formed (Fig. 3), WT maximum levels of Ca^{2+}_o -stimulated Ca^{2+}_i signaling were observed (Fig. 6B). The loss of Ca^{2+}_o potency points to complementary signaling via either the alternative *in-trans* molecular pathway between subunits and/or *in-cis* pathways within individual subunits.

It was not previously possible to exclude signaling *in-cis* for the CaSR. In the present study we tested for it by co-expressing (i) CaSR(G143E/L797A)₉₀₈-B2, which was defective in both its VFT-based Ca^{2+}_o -sensing and iL-3 signaling functions, and (ii) CaSR₈₇₅-B1, which had an intact VFT and a functionally competent signaling domain. Despite delivery of CaSR₈₇₅-B1 to the cell surface, the available *in-cis* pathway in this subunit was unable to support Ca^{2+}_o -stimulated Ca^{2+}_i mobilization (Fig. 6A). Thus, the responses were not supported by signaling *in-cis*.

Related class C GPCRs also exhibit signaling by *trans* conformational change. Previously, the glutamate analog quisqualate was found to activate both *in-trans* and *in-cis* dependent Ca^{2+}_i responses in mGlu₅-transfected HEK-293 cells.^(31,45) Whether CaSR-activating L-amino acids^(56,57); reviewed in Ref. 10) or one of the more potent amino acid analog activators of CaSR-mediated Ca^{2+}_i signaling (eg, S-methylglutathione⁽³⁸⁾ or L-1,2,3,4-tetrahydronorharman 3-carboxylic acid⁽²²⁾) might support *in-cis* signaling is unknown. Different activators and signaling pathways may require distinct intramolecular and intermolecular rearrangements associated with distinct requirements for *in-cis* or *in-trans* signaling within dimers, providing a basis for ligand-biased signaling^(36,58); reviewed in Ref. 59).

On the other hand, *in-cis* signaling clearly *does operate* within the CaSR's HH bundles (ie, beyond the C-termini of the dimeric VFT units), as highlighted by responses to the phenylalkylamine modulator NPS-R568, which binds in the CaSR's HH bundle.^(59,60) Thus, heterodimers, in which mutations were combined that impair either (i) the binding of phenylalkylamine positive modulators (E837A in TMD-6) or (ii) IP₁ accumulation (F801A in iL-3), retained NPS-R568-activated IP₁ accumulation if the two mutations were located in the same subunit but not if they were located in neighboring subunits.⁽¹¹⁾ Furthermore, the mGlu₂ positive modulator LY487379 and negative modulator MNI-136 respectively promoted or suppressed G_i binding to nanodiscs bearing monomeric mGlu₂.⁽¹²⁾

Hence *in-trans* signaling arising from VFT domain-dependent activation of the HH bundles is required for CaSR-mediated Ca^{2+}_o -stimulated Ca^{2+}_i mobilization. Recently reported cryoEM structure analysis of the inactive and active forms of near-to-full length CaSR including the entire extracellular domain, HH bundles, and shortened intracellular domains demonstrates that upon receptor activation, the HH bundles become closely apposed and rotate to form a new dimer interface formed by TMD-6:TMD-6'.^(14,61) Thus, within the dimeric VFT unit, each VFT domain engages with the HH bundle of its neighboring subunit along an expanded dimer interface that includes lobes 1 and 2 of

the VFT domains and the proximal region of the CR domains. These cross-subunit interactions would appear to contribute, at least in part, to *in-trans* signaling for Ca^{2+}_o -stimulated Ca^{2+}_i mobilization⁽¹⁷⁾ and the present study) and PI-PLC activation.⁽¹¹⁾

Uncertainty remains regarding the number of G protein binding sites per dimer and the nature of G protein activation will require solution of structures for protein complexes, such as CaSR-G_{q/11}. Based on observed asymmetry in one recently described active structure receptor,⁽¹⁴⁾ two G protein binding sites have proposed per receptor dimer, one associated with each subunit. According to this interpretation, G protein occupancy and activation alternate repetitively between the two HH bundles and their associated G protein sites. Our results for mutations of the VFT domain or iL-2/iL-3, or *in-trans* combinations are considered from this perspective in Fig. 7.

It might be wondered why heterodimers, in which G143E is present in one subunit and L797A is present in the other subunit, do not exhibit a reduction in maximum response to the level observed in heterodimers containing L797A; ie, to around 30%–40% of the WT maximum (Fig. 5). Although several scenarios are possible, it seems likely that this behavior arises from *in-trans partnering*, whereby the maximum response of the heterodimer is entirely dependent on the WT VFT domain in CaSR(L797A)₈₇₅-B1 partnering with the WT signaling domain in CaSR(G143E)₉₀₈-B2. One possible explanation is presented in Fig. 7.

Conclusions

In conclusion, we have developed a system that permits the expression of functionally competent CaSR heterodimers at the cell surface utilizing chimeras with the GABA_{B1/2} C-terminal sorting system. The system was used successfully to study the requirements of Ca^{2+}_o -stimulated signaling. Two functionally competent VFT domains were required to support WT levels of Ca^{2+}_i mobilization responses and a pronounced gene dosage effect was observed, whereby the loss of one functional VFT domain in mutant heterodimers impaired Ca^{2+}_o sensitivity but not the maximum response, and loss of function of both VFT domains abolished Ca^{2+}_o -stimulated Ca^{2+}_i mobilization. Two functionally competent G protein activating intraloops were also required to support WT levels of Ca^{2+}_o -stimulated Ca^{2+}_i mobilization. However, we did not observe a gene dosage effect for intraloop mutations. Thus, the loss of one functional intraloop (whether iL-2 or iL-3) markedly impaired maximal Ca^{2+}_o -stimulated Ca^{2+}_i mobilization and there was no further impairment in mutant heterodimers in which intraloops from both subunits were affected by the same mutation. Similar results were obtained for CaSR-mediated G_{q/11}-dependent PI-PLC. However, when one functional intraloop (whether iL-2 or iL-3) was present near total loss of signaling occurred. Finally, we found that Ca^{2+}_o -stimulated Ca^{2+}_i mobilization is exclusively supported by signaling *in-trans* between the VFT domain of one subunit to the HH bundle of its neighbor and is not supported by signaling *in-cis*. Thus, domain-based rearrangements upon Ca^{2+}_o binding to receptor dimers establish critical engagement between the VFT domains and HH bundles of neighboring subunits in support of Ca^{2+}_i mobilization and PI-PLC activation and, presumably, other forms of signaling. Future studies should investigate whether CaSR-targeting therapeutics might be used to correct impairments in signaling linked to disorders of calcium metabolism and whether their efficacy is dependent not only on

the locations of disorder-related mutations but also on whether they are heterozygous or homozygous in nature.

Acknowledgments

This study was supported by National Health and Medical Research Council of Australia Project Grants APP1085143 and APP1138891, and Australian Research Council Fellowship Grants FT160100075 (KL) and FT170100392 (KJG). We thank Mr Roy Chan BSc(Hons) for technical assistance with the methods in molecular biology, Mr Cameron Nowell for technical assistance with the acquisition of cell images, and Prof Arthur Christopoulos for stimulating discussions. Open access publishing facilitated by The University of Sydney, as part of the Wiley - The University of Sydney agreement via the Council of Australian University Librarians.

Author Contributions

Mahvash A. Goolam: Conceptualization; data curation; formal analysis; investigation; visualization; writing – original draft; writing – review and editing. **Alice P. Brown:** Investigation; methodology; visualization; writing – review and editing. **Kimberly Taynash Edwards:** Conceptualization; methodology; writing – review and editing. **Karen J. Gregory:** Investigation; methodology; resources; software; validation; writing – review and editing. **Katie Leach:** Data curation; formal analysis; funding acquisition; investigation; methodology; resources; software; validation; visualization; writing – review and editing. **Arthur David Conigrave:** Conceptualization; data curation; funding acquisition; investigation; methodology; project administration; resources; software; supervision; validation; visualization; writing – original draft; writing – review and editing.

Conflicts of Interest

None of the authors has any conflicts to declare.

Ethical Statement

The experiments described in this article were performed on cloned cDNAs encoding the human calcium-sensing receptor and mouse GABA_{B1} and human GABA_{B2} receptor subunits provided by colleagues and modified by genetic engineering techniques in vitro as described in the Methods section. The proteins encoded by control and modified cDNA constructs were expressed in a standard laboratory cell line, HEK-293. No animal or human subjects participated in the study.

Data Availability

The data that support the findings of this study are available from the corresponding author upon reasonable request.

References

1. Wingler L, Lefkowitz R. Conformational basis of G protein-coupled receptor signaling versatility. *Trends Cell Biol.* 2020;30:736-747.
2. Hilger D, Masureel M, Kobilka B. Structure and dynamics of GPCR signaling complexes. *Nat Struct Mol Biol.* 2018;25:4-12.

3. Wootten D, Christopoulos A, Marti-Solano M, Babu M, Sexton P. Mechanisms of signalling and biased agonism in G protein-coupled receptors. *Nat Rev Mol Cell Biol.* 2018;19:638-653.
4. Pin J, Kniazeff J, Prézeau L, Liu J, Rondard P. GPCR interaction as a possible way for allosteric control between receptors. *Mol Cell Endocrinol.* 2019;486:89-95.
5. Conigrave A. The calcium-sensing receptor and the parathyroid: past, present, future. *Front Physiol.* 2016;7(563):1-13.
6. Hannan F, Kallay E, Chang W, Brandi M, Thakker R. The calcium-sensing receptor in physiology and in calcitropic and noncalcitropic diseases. *Nat Rev Endocrinol.* 2018;15:33-51.
7. Leach K, Hannan F, Josephs T, et al. Calcium-sensing receptor nomenclature, pharmacology, and function. *Pharmacol Rev.* 2020;72:558-604.
8. Brown EM, MacLeod RJ. Extracellular calcium sensing and extracellular calcium signaling. *Physiol Rev.* 2001;81:239-297.
9. Brown E. Role of the calcium-sensing receptor in extracellular calcium homeostasis. *Best Pract Res Clin Endocrinol Metab.* 2013;27:333-343.
10. Conigrave A, Ward D. Calcium-sensing receptor (CaSR): pharmacological properties and signaling pathways. *Best Pract Res Clin Endocrinol Metab.* 2013;27:315-331.
11. Jacobsen S, Gether U, Bräuner-Osborne H. Investigating the molecular mechanism of positive and negative allosteric modulators in the calcium-sensing receptor dimer. *Sci Rep.* 2017;7:46355.
12. El Moustaine D, Granier S, Doumazane E, et al. Distinct roles of metabotropic glutamate receptor dimerization in agonist activation and G-protein coupling. *Proc Natl Acad Sci U S A.* 2012;109:16342-16347.
13. Vafabakhsh R, Levitz J, Isacoff E. Conformational dynamics of a class C G-protein-coupled receptor. *Nature.* 2015;524:497-501.
14. Gao Y, Robertson M, Rahman S, et al. Asymmetric activation of the calcium-sensing receptor homodimer. *Nature.* 2021;595:455-459.
15. Khan MA, Conigrave AD. Mechanisms of multimodal sensing by extracellular Ca²⁺-sensing receptors: a domain-based survey of requirements for binding and signalling. *Br J Pharmacol.* 2010;159:1039-1050.
16. Kniazeff J, Prézeau L, Rondard P, Pin J, Goudet C. Dimers and beyond: the functional puzzles of class C GPCRs. *Pharmacol Ther.* 2011;130:9-25.
17. Bai M, Trivedi S, Kifor O, Quinn SJ, Brown EM. Intermolecular interactions between dimeric calcium-sensing receptor monomers are important for its normal function. *Proc Natl Acad Sci U S A.* 1999;96:2834-2839.
18. Xue L, Rovira X, Scholler P, et al. Major ligand-induced rearrangement of the heptahelical domain interface in a GPCR dimer. *Nat Chem Biol.* 2015;11:134-140.
19. Nørskov-Lauritsen L, Jørgensen S, Bräuner-Osborne H. N-glycosylation and disulfide bonding affects GPRC6A receptor expression, function, and dimerization. *FEBS Lett.* 2015;589:588-597.
20. Kunishima N, Shimada Y, Tsuji Y, et al. Structural basis of glutamate recognition by a dimeric metabotropic glutamate receptor. *Nature.* 2000;407:971-977.
21. Muto T, Tsuchiya D, Morikawa K, Jingami H. Structures of the extracellular regions of the group II/III metabotropic glutamate receptors. *Proc Natl Acad Sci U S A.* 2007;104:3759-3764.
22. Zhang C, Zhang T, Zou J, et al. Structural basis for regulation of human calcium-sensing receptor by magnesium ions and an unexpected tryptophan derivative co-agonist. *Sci Adv.* 2016;2:e1600241.
23. Geng Y, Mosyak L, Kurinov I, et al. Structural mechanism of ligand activation in human calcium-sensing receptor. *Elife.* 2016;5:e13662.
24. Kaupmann K, Malitschek B, Schuler V, et al. GABA(B)-receptor subtypes assemble into functional heteromeric complexes. *Nature.* 1998;396(6712):683-687.
25. White JH, Wise A, Main MJ, et al. Heterodimerization is required for the formation of a functional GABA(B) receptor. *Nature.* 1998;396(6712):679-682.
26. Margeta-Mitrovic M, Jan Y, Jan L. A trafficking checkpoint controls GABA(B) receptor heterodimerization. *Neuron.* 2000;27:97-106.

27. Pollak MR, Chou YW, Marx SJ, et al. Familial hypocalciuric hypercalcemia and neonatal severe hyperparathyroidism. Effects of mutant gene dosage on phenotype. *J Clin Invest.* 1994;93:1108-1112.
28. Pearce SH, Bai M, Quinn SJ, Kifor O, Brown EM, Thakker RV. Functional characterization of calcium-sensing receptor mutations expressed in human embryonic kidney cells. *J Clin Invest.* 1996;98:1860-1866.
29. Bai M, Quinn S, Trivedi S, et al. Expression and characterization of inactivating and activating mutations in the human Ca²⁺-sensing receptor. *J Biol Chem.* 1996;271:19537-19545.
30. Hannan F, Babinsky V, Thakker R. Disorders of the calcium-sensing receptor and partner proteins: insights into the molecular basis of calcium homeostasis. *J Mol Endocrinol.* 2016;57:R127-R142.
31. Kniazef J, Bessis A-S, Maurel D, Ansanay H, Prezeau L, Pin J-P. Closed state of both binding domains of homodimeric mGlu receptors is required for full activity. *Nat Struct Mol Biol.* 2004;8:706-713.
32. Gregory KJ, Kufareva I, Keller AN, et al. Dual action calcium-sensing receptor modulator unmasks novel mode-switching mechanism. *ACS Pharmacol Transl Sci.* 2018;1:96-109.
33. Chang W, Chen TH, Pratt S, Shoback D. Amino acids in the second and third intracellular loops of the parathyroid Ca²⁺-sensing receptor mediate efficient coupling to phospholipase C. *J Biol Chem.* 2000;275:19955-19963.
34. Goolam M, Ward J, Avlani V, Leach K, Christopoulos A, Conigrave A. Roles of intraloops-2 and -3 and the proximal C-terminus in signalling pathway selection from the human calcium-sensing receptor. *FEBS Lett.* 2014;588:3340-3346.
35. Mun H, Culverston E, Franks A, Collyer C, Clifton-Bligh R, Conigrave A. A double mutation in the extracellular Ca²⁺-sensing receptor's Venus fly trap domain that selectively disables L-amino acid sensing. *J Biol Chem.* 2005;280:29067-29072.
36. Davey A, Leach K, Valant C, Conigrave A, Sexton P, Christopoulos A. Positive and negative allosteric modulators promote biased signalling at the calcium-sensing receptor. *Endocrinology.* 2012;153:1232-1241.
37. Stephanick A, McKenna J, McGovern O, Huang Y, Breitwieser GE. Calcium-sensing receptor mutations implicated in pancreatitis and idiopathic epilepsy syndrome disrupt an arginine-rich retention motif. *Cell Physiol Biochem.* 2010;26:363-374.
38. Broadhead G, Mun H, Avlani V, et al. Allosteric modulation of the calcium-sensing receptor by {gamma}-glutamyl peptides: inhibition of PTH secretion, suppression of intracellular cAMP levels and a common mechanism of action with L-amino acids. *J Biol Chem.* 2011;286:8786-8797.
39. Brennan S, Mun H, Leach K, Kuchel P, Christopoulos A, Conigrave A. Receptor expression modulates calcium-sensing receptor mediated intracellular Ca²⁺ mobilization. *Endocrinology.* 2015;156:1330-1342.
40. Reyes-Cruz G, Hu J, Goldsmith PK, Steinbach PJ, Spiegel AM. Human Ca²⁺ receptor extracellular domain. Analysis of function of lobe I loop deletion mutants. *J Biol Chem.* 2001;276:32145-32151.
41. Mun H, Leach K, Conigrave A. L-amino acids promote calcitonin release via a calcium-sensing receptor: Gq/11-mediated pathway in human C-cells. *Endocrinology.* 2019;160:1590-1599.
42. Ray K, Fan GF, Goldsmith PK, Spiegel AM. The carboxyl terminus of the human calcium receptor. Requirements for cell-surface expression and signal transduction. *J Biol Chem.* 1997;272(50):31355-31361.
43. Gama L, Breitwieser GE. A carboxyl-terminal domain controls the cooperativity for extracellular Ca²⁺ activation of the human calcium sensing receptor. A study with receptor-green fluorescent protein fusions. *J Biol Chem.* 1998;273(45):29712-29718.
44. Chang W, Pratt S, Chen TH, Bourguignon L, Shoback D. Amino acids in the cytoplasmic C terminus of the parathyroid Ca²⁺-sensing receptor mediate efficient cell-surface expression and phospholipase C activation. *J Biol Chem.* 2001;276:44129-44136.
45. Brock C, Oueslati N, Soler S, Boudier L, Rondard P, Pin JP. Activation of a dimeric metabotropic glutamate receptor by intersubunit rearrangement. *J Biol Chem.* 2007;282:33000-33008.
46. Bai M. Structure-function relationship of the extracellular calcium-sensing receptor. *Cell Calcium.* 2004;35:197-207.
47. Wetzschureck N, Lee E, Libutti SK, Offermanns S, Robey PG, Spiegel AM. Parathyroid-specific double knockout of Gq and G11 alpha-subunits leads to a phenotype resembling germline knockout of the extracellular Ca²⁺-sensing receptor. *Mol Endocrinol.* 2007;21:274-280.
48. Nesbit M, Hannan F, Howles S, et al. Mutations affecting G-protein subunit α 11 in hypercalcemia and hypocalcemia. *N Engl J Med.* 2013;368:2476-2486.
49. Chou YW, Pollak MR, Brandi ML, et al. Mutations in the human Ca²⁺-sensing receptor gene that cause familial hypocalciuric hypercalcemia. *Am J Hum Genet.* 1995;56:1075-1079.
50. Bai M, Trivedi S, Lane CR, Yang Y, Quinn SJ, Brown EM. Protein kinase C phosphorylation of threonine at position 888 in Ca²⁺-sensing receptor (CaR) inhibits coupling to Ca²⁺ store release. *J Biol Chem.* 1998;273:21267-21275.
51. Binmahfouz L, Centeno P, Conigrave A, Ward D. Identification of Serine-875 as an inhibitory phosphorylation site in the calcium-sensing receptor. *Mol Pharmacol.* 2019;96:204-211.
52. Lazarus S, Pretorius C, Khafagi F, et al. A novel mutation of the primary protein kinase C phosphorylation site in the calcium-sensing receptor causes autosomal dominant hypocalcemia. *Eur J Endocrinol.* 2011;164:429-435.
53. Hannan F, Nesbit M, Zhang C, et al. Identification of 70 calcium-sensing receptor mutations in hyper- and hypo-calcaemic patients: evidence for clustering of extracellular domain mutations at calcium-binding sites. *Hum Mol Genet.* 2012;21:2768-2778.
54. Hough TA, Bogani D, Cheeseman MT, et al. Activating calcium-sensing receptor mutation in the mouse is associated with cataracts and ectopic calcification. *Proc Natl Acad Sci U S A.* 2004;101:13566-13571.
55. Chow JYC, Estrema C, Orneles T, Dong X, Barrett KE, Dong H. Calcium-sensing receptor modulates extracellular Ca²⁺ entry via TRPC-encoded receptor-operated channels in human aortic smooth muscle cells. *Am J Physiol Cell Physiol.* 2011;301:C461-C468.
56. Conigrave AD, Quinn SJ, Brown EM. L-amino acid sensing by the extracellular Ca²⁺-sensing receptor. *Proc Natl Acad Sci U S A.* 2000;97:4814-4819.
57. Liu H, Yi P, Zhao W, et al. Illuminating the allosteric modulation of the calcium-sensing receptor. *Proc Natl Acad Sci U S A.* 2020;117:21711-21722.
58. Leach K, Sexton P, Christopoulos A, Conigrave A. Engendering biased signalling from the calcium-sensing receptor for the pharmacotherapy of diverse disorders. *Br J Pharmacol.* 2014;171:1142-1155.
59. Leach K, Gregory K, Kufareva I, et al. Towards a structural understanding of allosteric drugs at the human calcium-sensing receptor. *Cell Res.* 2016;26:574-592.
60. Miedlich SU, Gama L, Seuwen K, Wolf RM, Breitwieser GE. Homology modeling of the transmembrane domain of the human calcium sensing receptor and localization of an allosteric binding site. *J Biol Chem.* 2004;279:7254-7263.
61. Wen T, Wang Z, Chen X, et al. Structural basis for activation and allosteric modulation of full-length calcium-sensing receptor. *Sci Adv.* 2021;7:eabg1483.
62. Park J, Zuo H, Frangaj A, et al. Symmetric activation and modulation of the human calcium-sensing receptor. *Proc Natl Acad Sci U S A.* 2021;118:e2115849118.